Total loss sensitivities and allocated losses: Conceptual relations in radial distribution networks

Sustainable Energy, Grids and Networks 46 (2026) 102240

Contents lists available at ScienceDirect

Sustainable Energy, Grids and Networks

journal homepage: www.elsevier.com/locate/segan

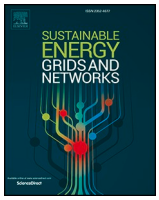

Total loss sensitivities and allocated losses: Conceptual relations in radial distribution networks

Soheil Saadatmandi, Andrea Mazza *, Gianfranco Chicco

Politecnico di Torino, Dipartimento Energia "Galileo Ferraris", Corso Duca degli Abruzzi 24, Torino 10129, Italy

ARTICLE INFO

Keywords:
Allocated losses-based product
Distribution system
Loss sensitivity
Planning scenario
Radial network
Reverse power flow

ABSTRACT

The sensitivity of distribution network losses to the change in net power at the network nodes (and phases of each node for unbalanced distribution systems) conveys key messages about the need to increase or decrease the net power to reduce network losses. Similar information is provided by the total network losses allocated to nodes and phases, determined based on the power flow solution. This paper provides original insights and new analytical formulations of the sensitivity of the total losses with respect to the node current magnitude for balanced and unbalanced radial distribution networks. Two novel fundamental results are presented: (i) the sign of the allocated losses is equal to the sign of total loss sensitivities with respect to the node current magnitudes, and (ii) the increase/reduction of the total losses for small net power changes in a node is identified by multiplying the sign of the allocated losses and the sign of the net node power, to obtain the allocated losses-based product, without carrying out further power flow calculations. Once established the relation between total loss sensitivities and allocated losses, the calculations are carried out by using the allocated losses, avoiding the need for assigning the directions of variation of power in the calculation of the sensitivities. The results are discussed on radial distribution systems with time-varying loads and generations and are used to establish novel losses-based strategies to assist distribution system operation and planning.

1. Introduction

With the progressive diffusion of distributed energy resources (DERs, with local generation, demand management and storage) in the distribution systems, the variety of operating conditions has considerably increased. For the analysis of distribution systems with DERs, the relevant point is the consideration of the *net load* (i.e., load minus generation) at the distribution system nodes [1]. The variability of the net load during time has a substantial impact on the distribution system operation, also requiring adjustments in the time scales for carrying out more accurate analyses [2]. The development of DERs can bring issues like overvoltage conditions appearing in some nodes of the system, branch loading limits exceeded, and reverse power flow (RPF) due to the injection of power into the supply system [3] from distribution networks [4]. These issues are identified through power flow calculations by using specific tools [5]. Moreover, the analysis of the distribution system operating conditions under various DER development scenarios can be useful in planning studies, to provide guidance on the evolution of the distribution system infrastructure depending on the installation of new DERs in the system [6], also by determining the hosting capacity [7].

To tackle the above-mentioned issues, the net load at the distribution system nodes can be modified to some extent, aiming at avoiding constraint violations, based on assessments of the extent and timings of the possible violations [8]. On the operation side, the programmable local generation can be scheduled appropriately, while non-programmable local generation (e.g., from renewable energy sources) can be curtailed as needed to preserve operational security [9]. On the demand side, deferrable (in time) and curtailable (in amplitude) demand can be considered in demand response programs based on the voluntary participation of the users [10]. Possible storage solutions may impact on the net load during charging and discharging, subject to the related constraints [11].

In the situations indicated above, changes in the net load can be driven by different factors. The nature of these factors can be:

- technical (e.g., to enhance the effectiveness of distribution system operation);
- economic (e.g., driven by electricity prices, or depending on incentives to provide grid services, also through the participation in demand response programs);

* Corresponding author.
E-mail addresses: soheil.saadatmandi@polito.it (S. Saadatmandi), andrea.mazza@polito.it (A. Mazza), gianfranco.chicco@polito.it (G. Chicco).

https://doi.org/10.1016/j.segan.2026.102240
Received 20 October 2025; Received in revised form 28 February 2026; Accepted 29 March 2026
Available online 30 March 2026

List of Acronyms

ALP	Allocated Losses-based Product
BCDLA	Branch Current Decomposition for Loss Allocation
DER	Distributed Energy Resource
DSO	Distribution System Operator
GSV	Global Sensitivity of Voltage
LSP	Loss Sensitivity-based Product
PV	Photovoltaic
RCLP	Resistive Component-based Loss Partitioning
RPF	Reverse Power Flow

List of SymbolsSubscripts

{a,b,c}	phases of the three-phase system
S	shunt
b	branch
k	node
p	phase
t	time step
tot	total

Superscripts

T	transposition operator
base	base case
new	new case for comparison

Sets

$\mathbb{B}_k$	set of the branches included in the path from node k to the slack node
$\mathbb{K}_b$	set of the nodes isolated by opening branch b

Variables

B	number of branches
I	current
K	number of nodes
P	active power
Q	reactive power
R	resistance
S	apparent power
V	voltage
X	reactance
δ	voltage angle
γ	current angle
λ	losses allocated
π	sensitivity-based product
σ	sensitivity coefficient
ξ	loss sensitivity
ζ	allocated losses-based product
$\mathscr{L}$	losses

Matrices and vectors

$\mathbf{I}$	current matrix
$\mathbf{L}$	branch-to-node incidence matrix
$\mathbf{\Gamma}$	inverse of the matrix $\mathbf{L}$
$\mathbf{R}$	resistance matrix
$\mathbf{Y}$	admittance matrix
$\mathbf{Z}$	impedance matrix
$\mathbf{1}$	vector with all unity values
$\mathbf{c}$	column vector
$\mathbf{i}$	current vector
$\boldsymbol{u}$	vector with a single unity component
$\mathbf{v}$	voltage vector
$\boldsymbol{\lambda}$	vector of the losses allocated to the three phases

- environmental (subject to related constraints on the global emission of greenhouse gases or on the local emission of hazardous pollutants, linked to economics through the corresponding penalties);
- social (e.g., depending on the participation of the users to energy communities or on the willingness to increase fairness in the management of the local generation).

As the benefits of changing the net load refer to the distribution system, the entity that manages the possible net load changes can be the distribution system operator (DSO) or an aggregator having a global view of the network and users. This entity can be the same that manages situations leading to curtailment of the generation from renewable energy sources, or demand response programs, or in general provision of grid services.

By focusing on the technical factors, improving the effectiveness of the distribution system operation traditionally requires reducing the network losses. The loss reduction objective is also consistent with the improvement of the voltage profile and with better balancing the branch loading.

The calculation of loss sensitivities with respect to the net power variation is an effective way to determine viable directions of loss reduction, by identifying whether loss reduction can be obtained through increasing or decreasing the net load. On the other hand, the loss allocation to the distribution system nodes can provide useful hints in the same direction, provided that a specific link between loss allocation and loss sensitivity can be found (this link, not available in the literature yet, is presented for the first time in this paper). A more focused view on loss sensitivity calculations and loss allocation based on selected contributions is presented below.

1.1. Loss sensitivity calculations

Starting from the power flow solution at a given time, sensitivity analysis is useful to provide information on the effects of a small change in each input on the distribution system operation. Traditional calculations consider the sensitivity of the total system losses with respect to the variation of a given input (e.g., active or reactive power generation or demand in a network node) [12]. For this purpose, loss sensitivity factors have been defined based on the linearisation of the non-linear exact loss formula [13] to determine how sensitive the system losses are to the real or reactive power injection at any bus [14]. The analytical loss sensitivity calculations proposed in [15] are based on tracking the changes of the complex power of a line connected to the node where the change of the complex power occurs. The sensitivities calculated refer to network losses and voltage variations. The power loss estimation method proposed in [16] is based on second-order power flow sensitivities, which can represent the non-linear nature of the power losses.

In the fast sensitivity method for determining line loss and node voltages in active distribution network proposed in [17], a quadratic sensitivity model of branch losses to distributed generation output or load and a linear sensitivity model of node voltages to distributed generation output or load are formulated based on an initial power flow solution. Linearised expressions of the branch losses have been introduced in [18] by using loss sensitivity factors calculated from the power flow solution.

All the sensitivity formulations indicated above refer to balanced systems. However, distribution systems generally operate under unbalanced conditions, and in some cases also their structure is not symmetric and needs to be represented with specific formulations, such as resorting to the determination of self-impedances and mutual impedances by

using the Carson equations [19]. For unbalanced distribution systems, sensitivity calculations have been conducted in [20] with an approximate method in which the power losses in every branch are computed in a matrix form. The approach presented considers a demand change at a given node and phase, with a set of assumptions concerning non-significant changes occurring in both the currents of the other nodes and in the other phases at the same node subject to the demand change. Significant changes are considered only for the phase currents at the upstream branches that connect the node to the slack. A sensitivity matrix for the voltage unbalance factor has been formulated in [21] by considering variations in the unbalanced power inputs of single-phase and three-phase loads.

Recent research trends have introduced data-driven approaches, in which the determination of sensitivities has been incorporated in the solution processes. Voltage sensitivities with respect to active power and reactive power variations have been typically considered in most references (e.g., [22–27]). In particular, sensitivity calculations have been developed in [22] to find the impact of uncertainty of the inputs from loads and photovoltaic systems to the distribution system node voltages; the calculation of Sobol indices provides the most significant inputs that have an impact on voltage variations. The global sensitivity of voltage (GSV) has been combined in [23] with multi-agent adversarial learning to obtain a robust control policy in a distribution system with deep penetration of photovoltaic generators. Voltage sensitivities with respect to real/reactive power injections have been predicted in [24] by using a deep neural network that takes the bus active and reactive power injections and voltages as inputs. A sensitivity gate designed to use voltage sensitivity data has been proposed in [25] to improve the performance of the model established for determining the hosting capacity in distribution networks. The voltage sensitivity data used is determined by computing the voltage variation at the other buses when adding a unit of generation at one bus. A data-driven sparse estimator of voltage sensitivities has been proposed in [26] for large-scale distribution systems with photovoltaic generation, robust to photovoltaic stochasticity and measurement noise. The sensitivities of some three-phase unbalance metrics with respect to the power injections have been addressed in [27]. However, none of the previous references indicated for the data-driven approaches addresses loss sensitivities.

Loss sensitivity calculations can be applied to various problems. Some examples addressed in the distribution systems literature are the reduction of the power losses by choosing the optimal locations of different types of distributed energy resources (in [14] and [16]) and the improvement of the clearing mechanism in local markets by reflecting the loss variation (in [18], and in [28] by using the method defined in [20]). An overview of different methods with a list of potential applications can be found in [12].

Table 1 shows the different aspects considered in the loss sensitivity calculations, taking selected references to represent the various types of contributions and anticipating the aspects related to the proposed approach. The details of the formulations used are different in all the papers. The research gaps are summarised in the next subsection.

1.2. Losses allocated to the system nodes

Another line of research has provided specific formulations for allocating the total distribution system losses to the system nodes. Initial pro-rata schemes [29], based on linear or quadratic proportions of the allocated losses with respect to the loads at the nodes, are not suitable to be applied in a system with DERs. In fact, with DERs the relevant entry is the *net power* at the node, determined as the difference between the load power and the local generation power, which can be positive or negative, while pro-rata schemes are applied to positive values only. In the presence of storage, charging is seen as a load and discharging as a local generation.

The key point of the allocated losses is that their sum must be equal to the total network losses. The allocated losses can be positive or negative, and their sign may incorporate useful information on the need for augmenting or reducing the net power in the area where the node is located. This property is not directly available in methods for marginal loss allocation [30], which also require normalisation to encompass non-linearities. Likewise, loss allocation has been addressed in [31] by using two methods, called Marginal Loss Coefficients and Direct Loss Coefficients, based on the derivatives of the power flow equations, resorting to the use of some entries of the Jacobian and Hessian matrices of the power flow equations. In these methods, the losses allocated to the nodes are determined by multiplying the loss coefficients and the node power. In both cases, the total allocated losses are not guaranteed to be exactly equal to the total network losses in any condition. Therefore, a reconciliation procedure based on the normalisation of the loss coefficients is needed to obtain equality between total allocated losses and total network losses.

Furthermore, flow-tracing methods based on the linear proportional sharing principle [32] have been formulated, which allocate the losses either to generators or loads [33]. The flow-tracing methods are based on the linear proportional sharing principle. As also discussed in [34], to allocate losses to the demands, the losses of a line reaching a given node are assigned to the (other) lines and demands connected to that node proportionally to their power flow. In this way, all losses would be allocated to the demands. On the other side, the same principle can be used for allocating losses to generators, associating the losses of a line whose flow leaves a node to the lines whose flow enters the node (or to the generation in that node) proportionally to their power flows. In this way, all losses would be allocated to generators. If both loads and generators are present, losses are first allocated to demands and then to generators. Then, 50% of the losses are assigned to the generation and 50% to the demand and the allocated losses are recalculated for generations and demands. The result is that the total allocated losses are equal to the total losses, and the allocated losses are never negative. This approach uses only the line losses and the active power flows and is generally applicable to meshed networks. In this respect, while in transmission systems the losses can be allocated to all generators, in distribution systems the slack node is not a physical node. Thus, the slack node must be excluded from the loss allocation mechanism [35], with a direct impact on the application of the proportional sharing principle, especially in the presence of RPF. In any case, in the presence

Table 1
Loss sensitivity calculations – representative contributions from the state of the art.

Ref.	Loss sensitivity w.r.t.			Balanced system		Sensitivity formulation		
	power	voltage	current	Yes	no	linearised	non-linear	2nd order
[12]	√			√		√		
[15]	√			√			√	
[16]		√		√				√
[17]	√			√			√	
[18]		√		√		√		
[20]	√			√	√		√	
This paper			√	√	√		√	

of loads and local generators in distribution systems the flow-tracing method suffers from the equal partitioning of the allocated losses between the total demand and the total generation, which cannot capture local aspects depending on the positive or negative net power in the network nodes.

On the other hand, circuit-based methods have been developed without calculating the derivatives of the power flow equations, by directly determining the allocated losses rather than the loss allocation factors. In the circuit-based methods, the calculation of the allocated losses is based on the net current inputs to the nodes. By definition of these methods, the total allocated losses are equal to the total network losses. Two circuit-based methods, formulated for both transmission and distribution networks, are the $\mathbf{Z}_{\text{bus}}$ method [36], based on the bus impedance matrix $\mathbf{Z}_{\text{bus}}$, and the modified $\mathbf{Y}_{\text{bus}}$ method [37], based on the bus admittance matrix $\mathbf{Y}_{\text{bus}}$. The $\mathbf{Z}_{\text{bus}}$ method can be applied to distribution networks by directly connecting the slack node to the reference node [35]. For radial distribution systems, dedicated methods have been developed. For balanced systems, the Branch Current Decomposition for Loss Allocation (BCDLA) [38] formulated the allocated losses in an analytical way starting from the expression of the Joule losses in the network branches. The paper also discusses why appropriate starting expressions for loss allocation purposes use the branch resistance only. In fact, the formulation of the branch losses using the product of the voltage drop in the branch times the branch current may lead to a reactive power paradox with the allocation of higher losses to the node with lower reactive power when the active power of the node is the same, depending on the characteristic angles of the load and of the branch impedance. The BCDLA method provides the allocated losses without requiring any further action. It is different from other approaches (such as in [39,40] and [41]) where some cross-terms appear at a certain stage of the calculations and hence user-defined rules have to be adopted to complete the loss allocation process, or from the solution given by cooperative game problems based on the Shapley value [42] or the τ-value [43]. Finally, the BCDLA method does not address economics, while in other cases the allocated losses are normalised with respect to the total loss costs [44] and graph-based techniques are used for loss allocation in transactive energy markets [45] tracing the evolution of the transactions during time [46].

For three-phase unbalanced systems with neutral modelled according to the Carson equations [19], the Resistive Component-based Loss Partitioning (RCLP) method [47] has been formulated by starting from the representation of the Joule losses. The expressions used in the BCDLA and RCLP approaches are recalled in Section 2.2. Another development for unbalanced systems is presented in [48], where the neutral conductor is treated separately, but user-defined assumptions are needed to assign the weighting factors to the cross-terms of different phase currents. In [47] it is also discussed the loss partitioning paradox, which refers to the use of the branch impedance matrix in the loss allocation formula. In this case, for the same three-phase branch losses, the losses allocated to the phases could be very different (even very high and negative on different phases). The loss partitioning paradox is eliminated by using the RCLP formulation of the branch losses based on the branch resistance matrix only. The RCLP approach is then used in this paper for loss allocation in unbalanced distribution systems.

In three-phase unbalanced distribution systems, the components are represented in detailed ways, with specific representations for distribution system transformers and DERs [49]. The calculation of the allocated losses starts from the power flow solution, in which node and branch currents are available for any kind of model used. Using the above-mentioned analytical formulations, the computation time to obtain the allocated losses is substantially negligible with respect to the time needed for the power flow solution.

1.3. Research gaps, contributions and paper organisation

To the authors' knowledge, the main research gaps realised after the analysis of the technical literature are as follows:

- The representation of the loads with the constant power model is traditional and purely conventional, as there is basically no load that behaves exactly as a constant power when the node voltage changes. In addition, the constant power model in most cases assumes that the reactive power to active power ratio is constant, which is another conventional yet arbitrary position, often far from reality.
- Loss sensitivity formulations mainly refer to balanced systems. The existing methodology for determining the sensitivity of the total network losses with respect to the variation of the local generation or demand in unbalanced cases is affected by the presence of limiting assumptions.
- The allocated losses are formally different with respect to the loss sensitivities, even though some properties of the allocated losses (e.g., the sign) may be useful to identify cases in which an increase of the local load could determine a reduction in the total network losses. Yet, the relation between the losses allocated to the network nodes and the loss sensitivity entries has not been fully clarified so far.

This paper aims at addressing the research gaps indicated above by presenting some novel findings and analyses specifically formulated for radial distribution systems.

The main novelties of this paper are:

1. Determining for the first time analytical expressions of total loss sensitivity with respect to the node current magnitude for three-phase balanced and unbalanced systems. The expressions are obtained starting from the formulations of the allocated losses that give the exact total network losses. This novel formulation avoids the need to consider some limiting assumptions introduced in the state of the art.
2. Clarifying for the first time the relation between the losses allocated to the network nodes and the loss sensitivity entries for balanced and unbalanced systems.
3. Introducing for the first time a simple and effective way to determine analytically whether the total network losses increase or decrease after a small variation of the net power at a given node (and phase for an unbalanced system) without executing additional power flow calculations.
4. In addition, the findings obtained from the proposed approach are used to formulate a new benchmark scenario for assessing the impact of adding new photovoltaic (PV) generation on the distribution system losses.

For radial distribution systems, the power flow is calculated by using the backward/forward sweep method, easy to implement and with good convergence properties [50], also adaptable to weakly-meshed networks [51]. The losses are allocated to the nodes and not to the individual local load or generation connected to the node. Hence, the allocated losses refer to the net load and *not* to the individual DER components connected to the node. The testing of the proposed approach is carried out by analysing both balanced and unbalanced distribution systems, considering the variation in time of loads and local generations.

The next sections of this paper are organised as follows. Section 2 sets up the framework of analysis concerning the calculations of sensitivities and allocated losses. Section 3 provides an interpretation of the meaning of the total loss sensitivities and allocated losses. New indicators, calculated starting from the power flow solution, are determined to reach new fundamental results in the interpretation of the relations between sensitivity and allocated losses. Section 4 presents and discusses some significant application cases for balanced and unbalanced distribution systems. The last section contains the concluding remarks.

2. Determination of the sensitivity of the network losses with respect to the net load variation and of the losses allocated to the nodes

2.1. Notation for the radial distribution system

The radial distribution network considered is supplied from the slack node (denoted with the number 0) and contains other K nodes with local generation and/or load, and B branches. The branches are numbered with the same number of the receiving node (which in the radial system is unique). The distribution system is represented by using the branch-to-node incidence matrix $\mathbf{L}$ (in which the entries for each branch are -1 for the sending node and 1 for the ending node) and its inverse matrix $\mathbf{\Gamma} = \mathbf{L}^{-1}$. The matrix $\mathbf{\Gamma}$ has interesting properties: the non-null entries in row $k = 1, \ldots, K$ indicate the branches that belong to the path from node k to the slack node (included in the set $\mathbb{B}_k$), and the non-null entries in column b indicate the nodes isolated by opening branch $b = 1, \ldots, B$ (included in the set $\mathbb{K}_b$, while the b^{th} column of the matrix $\mathbf{\Gamma}$ is denoted as $\mathbf{c}_b$).

The structure of the distribution network is considered by separating the longitudinal parameters (series impedance of the branch) from the contribution to the shunt node currents (depending on the shunt parameters of the branches,[1] the net load complex power given as the difference between the complex power of the load and the complex power of the local generation, and the reactive power from compensation devices). The series parameters of the branch $b = 1, \ldots, B$ are the resistance R_b and the reactance X_b.

For the study presented in this paper, the steady-state calculations are carried out considering a succession of $t = 1, \ldots, T$ time steps. Let us further denote as $\mathscr{L}_{\text{tot},t}$ the total network losses at time step t.

For a *balanced* system, at each time step and node $k = 1, \ldots, K$, the difference between the average power of local load and local generation is denoted as $P_{k,t}$ for the net active power and $Q_{k,t}$ for the net reactive power. The power flow solution yields the bus voltage $\overline{V}_{k,t} = V_{k,t}e^{j\delta_{k,t}}$ and the shunt node current $\overline{I}_{\text{Sk},t} = I_{\text{Sk},t}e^{j\gamma_{\text{Sk},t}}$ at node $k = 1, \ldots, K$, also expressed in vector form as $\mathbf{i}_{\text{S},t} = \left[\overline{I}_{\text{S1},t} \ldots \overline{I}_{\text{SK},t}\right]^{\text{T}}$. The branch currents for branch $b = 1, \ldots, B$ are determined as $\overline{I}_{b,t} = \sum_{k\in\mathbb{K}_b} \overline{I}_{\text{Sk},t}$.

For an *unbalanced* system, let us denote the three phases as {a,b,c} and use the variable p to indicate a generic phase. The shunt node currents in the three phases of node $k = 1, \ldots, K$ are expressed as $\overline{I}_{\text{Sk},p,t} = I_{\text{Sk},p,t}e^{j\gamma_{\text{Sk},p,t}}$ and are combined in the vector $\mathbf{i}_{\text{Sk},t} = \left|\overline{I}_{\text{Sk,a},t} \quad \overline{I}_{\text{Sk,b},t} \quad \overline{I}_{\text{Sk,c},t}\right|^{\text{T}}$. In turn, the shunt node current vectors are included in the matrix $\mathbf{I}_{\text{S},t} = \left|\mathbf{i}_{\text{S1},t} \quad \ldots \quad \mathbf{i}_{\text{SK},t}\right|$. The branch current vectors for branch $b = 1, \ldots, B$ are determined as $\mathbf{i}_{b,t} = \sum_{k\in\mathbb{K}_b} \mathbf{i}_{\text{Sk},t}$. The distribution network model considers the Carson equations to determine the self-impedances and mutual impedances of each branch $b = 1, \ldots, B$, which, after applying the Kron reduction, is represented with a 3×3 matrix denoted as $\mathbf{Z}_{b,\text{abc}}$, with real part $\mathbf{R}_{b,\text{abc}} = \mathscr{R}e\{\mathbf{Z}_{b,\text{abc}}\}$ [52].

Finally, for the matrix representations used below, let us define the vectors $\mathbf{1}_3 = \left|1 \quad 1 \quad 1\right|^{\text{T}}$ referring to the three phases and $\mathbf{1}_K = \left|1 \quad \ldots \quad 1\right|^{\text{T}}$ with K components equal to unity referring to K nodes.

2.2. Identification of the RPF conditions

To identify the occurrence of RPF conditions, the current magnitude alone is unable to capture the direction of the current. Using further information, e.g., on the sign of the net power, is needed.

Starting from a power flow solution, the identification of the occurrence of RPF can be carried out in different ways. For a *balanced* system, the RPF towards the supply system is detected when there is a negative entry in the real part of the complex power $\overline{S}_0$ injected into the grid. Alternatively, the current taken from the supply grid is calculated by considering[2] the angle γ_0 of the current $\overline{I}_0 = \overline{S}_0^*/\overline{V}_0^*$, from which the RPF conditions occur when the angle displacement $|\delta_0 - \gamma_0| > \pi/2$, with the angle δ_0 of the slack node $\overline{V}_0$, typically $\delta_0 = 0$.

For an *unbalanced* system, the RPF conditions are determined at each phase, as RPF could occur at one phase or two phases only. Again, the RPF conditions occur when the real part of the complex power $\overline{S}_{0p}$ injected into the grid at phase p is negative, or the angle displacement $\delta_{0p} - \gamma_{0p}$ of the current $\overline{I}_{0p} = \overline{S}_{0p}^*/\overline{V}_{0p}^*$ with respect to the slack node voltage $\overline{V}_{0p}$ at phase p satisfies the condition $\left|\delta_{0p} - \gamma_{0p}\right| > \pi/2$.

2.3. Losses allocated to the nodes

For balanced distribution systems, the losses allocated to node $k = 1, \ldots, K$ from the BCDLA approach at time step t are determined as [38]:

$$\lambda_{k,t} = \mathscr{R}e\left\{\overline{I}_{\text{Sk},t}^* \sum\nolimits_{b\in\mathbb{B}_k} \left(R_b\, \overline{I}_{b,t}\right)\right\} \tag{1}$$

and the total losses allocated to the nodes, equal to the total network losses, are:

$$\mathscr{L}_{\text{tot},t} = \sum\nolimits_{k=1}^{K} \lambda_{k,t} \tag{2}$$

For unbalanced distribution systems, the vectors $\boldsymbol{\lambda}_{k,t}$ of the losses allocated to the three phases of node $k = 1, \ldots, K$ from the RCLP approach at time step t are determined as [47]:

$$\boldsymbol{\lambda}_{k,t} = \mathscr{R}e\left\{\mathbf{i}_{\text{Sk},t} \otimes \sum\nolimits_{b\in\mathbb{B}_k} \left(\mathbf{R}_{b,\text{abc}}\mathbf{i}_{b,t}^*\right)\right\} \tag{3}$$

where the symbol $\otimes$ indicates the component-by-component (or Hadamard) product. The sum of the losses allocated to each phase of each node are equal to the total network losses:

$$\mathscr{L}_{\text{tot},t} = \sum\nolimits_{k=1}^{K} \mathbf{1}_3^{\text{T}}\, \boldsymbol{\lambda}_{k,t} \tag{4}$$

2.4. Sensitivity calculations

The sensitivity of the total distribution network losses with respect to the change of active power at node $k = 1, \ldots, K$ is conceptually defined by the derivative $\partial\mathscr{L}_{\text{tot},t}/\partial P_{k,p,t}$. The same definition with derivative $\partial\mathscr{L}_{\text{tot},t}/\partial Q_{k,p,t}$ holds by considering the change of reactive power.

The practical approach for determining and interpreting the sensitivity starts from the power flow solution as the base case with total losses $\mathscr{L}_{\text{tot},t}^{(\text{base})}$ and changes the net load power (active power, in this example[3]) at phase p of node k from $P_{k,p,t}^{(\text{base})}$ to $P_{k,p,t}^{(\text{new})}$. In the new power flow solution, the total losses become $\mathscr{L}_{\text{tot},t}^{(\text{new})}$, and the sensitivity coefficient is calculated as:

$$\sigma_{k,p,t} \cong \frac{\mathscr{L}_{\text{tot},t}^{(\text{new})} - \mathscr{L}_{\text{tot},t}^{(\text{base})}}{P_{k,p,t}^{(\text{new})} - P_{k,p,t}^{(\text{base})}} \tag{5}$$

To obtain a total loss reduction, there are two cases: (*i*) the net power is reduced and sensitivity coefficient $\sigma_{k,p,t}$ is positive, or (*ii*) the net power increases and $\sigma_{k,p,t}$ is negative. The net power can be varied by changing either the load or the generation, namely, by reducing or increasing

[1] For low-voltage systems, the shunt parameters may be neglected.

[2] The voltage $\overline{V}_0$ is typically assumed as the angle reference for the entire system, with null voltage angle. The expression written here is the general one, in which the voltage angle δ_0 could be non-zero, as it may happen for example when studying integrated transmission and distribution systems.

[3] Sensitivities can be defined in a similar way for reactive power changes.

either load or generation with respect to the base case.

As indicated in Section 1.3, the use of the constant power model is not fully realistic and as such cannot be seen as an invariable reference from the state of the art. Because of that, in this paper a different reasoning is followed to define an analytical formulation of the sensitivities referring to the total losses. The sensitivity of the total losses is determined with respect to the node current magnitude, rather than with respect to active or reactive power. The determination of the sensitivity starts from the power flow solution and from the analytical equation that gives the total allocated losses, namely, Eq. (2) in the balanced case and Eq. (4) in the unbalanced case. The derivatives of the total losses are then computed with respect to the magnitude of one shunt node current at a time, keeping in every case constant angles of the currents. In this way, the change is not only related to variation of the load active or reactive power, because it also incorporates the contribution of the shunt branch parameters to the shunt node current. However, it has to be considered that the impact of the variation in the contributions to the shunt node current of the shunt branch parameters for a very small change in the load current is remarkably small (and even null in the case of distribution systems with null shunt admittance in the model).

When there is a load variation in a node, there are always two contents to consider, for example active and reactive power, or apparent power and power factor, or amplitude and angle of the current, or resistive and reactive parameters of the impedance. In real cases, for a generic load, the direction of change of active and reactive power is generally undetermined, while for calculating the sensitivities a direction of change must be established. As such, the assumption of considering the shunt node current magnitude as the relevant term for sensitivity calculations instead of active and reactive power, keeping the shunt current angles constant, is considered appropriate. A clear advantage of this assumption is that the shunt node current used for calculating the derivatives is directly available from the power flow solution computed with the backward/forward sweep approach. A further advantage is that both the calculated sensitivity and the losses allocated to the node refer to the same shunt node current. Because of that, it is possible to use the relations that define the allocated losses as the starting point for determining the sensitivities.

The novel analytical formulations of the sensitivity of the total losses with respect to the shunt node current magnitude are expressed as follows:

i. For the three-phase balanced system (the deduction of the formula is shown in Appendix A):

$$\xi_{k,t} = \frac{\partial \mathscr{L}_{\text{tot},t}}{\partial I_{\text{Sk},t}} = \sum\nolimits_{b\in\mathbb{B}_k} 2R_b \mathbf{c}_b^{\text{T}} \Re\text{e}\left\{\text{e}^{-\text{j}\gamma_{\text{Sk},t}} \mathbf{i}_{\text{S},t}\right\} \tag{6}$$

ii. For the three-phase unbalanced system, the analytical formulation is constructed by using the extended representation of each branch with the 3 × 3 matrix indicated in Section 2.1. The angle reference is the angle of the slack voltage at phase a, $\delta_{0\text{a}} = 0$. The angle of the shunt node current at phase p in the system reference is indicated as $\gamma_{\text{Sk},p,t}$. The vector $\mathbf{u}_p^{\text{T}}$ contains one entry equal to unity for the phase with respect to which the sensitivity is calculated, and zero otherwise, namely, $\mathbf{u}_{\text{a}}^{\text{T}} = |1\ \ 0\ \ 0|$, $\mathbf{u}_{\text{b}}^{\text{T}} = |0\ \ 1\ \ 0|$, and $\mathbf{u}_{\text{c}}^{\text{T}} = |0\ \ 0\ \ 1|$. Following the same deduction carried out in the balanced case, the analytical formulation of the total loss sensitivities with respect to the shunt node current magnitude at node k and phase p is written as:

$$\begin{aligned}\xi_{k,p,t} &= \frac{\partial \mathscr{L}_{\text{tot},t}}{\partial I_{\text{Sk},p,t}} \\ &= \mathbf{1}_3^{\text{T}} \left(\sum\nolimits_{b\in\mathbb{B}_k} \left[diag\left(\mathbf{u}_p^{\text{T}} \left(\mathbf{R}_{b,\text{abc}} + \mathbf{R}_{b,\text{abc}}^{\text{T}} \right) \right) \Re e\{ e^{-\text{j}\gamma_{\text{Sk},p,t}} (\mathbf{1}_3 \right.\right. \right. \\ &\quad \left.\left.\left. \bullet \mathbf{c}_b^{\text{T}}) \otimes \ \mathbf{I}_{\text{S},t} \} \right] \right) \mathbf{1}_K \end{aligned} \tag{7}$$

Eq. (7) is the version of Eq. (6) extended to three-phase systems. Starting from Eq. (4), the derivative of the total losses with respect to $I_{\text{Sk},p,t}$ is organised by introducing the vectors $\mathbf{1}_3^{\text{T}}$ and $\mathbf{1}_K$ to write in a compact form the equations of the three phases, since the intermediate part yields a $3 \times K$ matrix whose entries must be summed up together to reach the result. The three-phase version of the term $2R_b$ that appears in Eq. (6) is the sum of the branch resistance matrix and of its transpose, which encompasses the possibility that the branch structure is not symmetrical. The product $\mathbf{u}_p^{\text{T}} \left(\mathbf{R}_{b,\text{abc}} + \mathbf{R}_{b,\text{abc}}^{\text{T}} \right)$ gives a row vector that is then transformed into a diagonal matrix by using the operator "diag". The Hadamard product $(\mathbf{1} \bullet \mathbf{c}_b^{\text{T}}) \otimes \mathbf{I}_{\text{S},t}$ selects only the columns of the shunt current matrix corresponding to the non-null entries of the vector $\mathbf{c}_b$ (i.e., the nodes downward branch b). The term $\text{e}^{-\text{j}\gamma_{\text{Sk},p,t}}$ is scalar and has been found with the application of the symmetry properties of the cosine indicated in Appendix A.

3. Interpretation of the link between total loss sensitivities and allocated losses

This section describes for the first time, in a systematic way, the link that exists between the allocated losses and the total loss sensitivities for balanced and unbalanced radial distribution systems. A key aspect is that, with the formulation illustrated in this paper, the interpretation of the conceptual relationship is valid also in RPF conditions.

3.1. Findings referring to the total loss sensitivities – balanced system

To set up the main points of the reasonings, specific details are provided with reference to a simple example. Extended results obtained on balanced and unbalanced three-phase systems are then shown in Section 4.

The simple example refers to the three-node structure shown in Appendix A (Fig. A1). The system data correspond to a balanced low-voltage system with rated voltage 400 V and total load power lower than 100 kVA. For the sake of simplicity, the system has three equal branches (underground cable lines with cross-section 50 mm^2 and length 70 m each). For per unit (pu) calculations, considering the base voltage 400 V and the base power 100 kVA, the base impedance is 1.6 Ω and the base current is 144.3 A. The impedance of each branch is then 0.021 +j 0.0034 pu. In the notation, the calculations refer to a given time step t. The shunt admittances of the branches are null, so the shunt net power is equal to the net load power.

Let us first compare two cases with identical load power 0.1 +j0.05 pu at nodes 1 and 3, while the load power at node 2 changes with reactive power to active power ratio constant and equal to 0.5. Case 1 has 0.4 pu of net load power at node 2 and positive entries of the complex power injected in the grid (0.6090 +j0.3014 pu), while in Case 2 the net load power at node 2 is $P_{\text{S2},t}$ = -0.4 pu, which corresponds to the generation of enough power to supply the other loads and send the excess of generation as RPF through the slack node (the complex power injected in the grid is $\overline{S}_{0,t}$ = -0.1966-j0.0995 pu and has a negative real part).

The results referring to these two cases are shown in Table 2. In both cases, the *sign* of the allocated losses is *equal* to the *sign* of the corresponding total loss sensitivity terms. The numerical values are different basically because the sum of the allocated losses has to be equal to the

Table 2
Numerical results for the three-node balanced case (values in per units, base voltage 400 V, base power 100 kVA).

Case	Node # or branch #	Voltage	Shunt node current	Branch current	Total loss sensitivity w.r.t. node shunt current magnitude	Allocated losses	Total losses
1 (no RPF)	1	$0.9913\ e^{j0.0027}$	$0.1128\ e^{-j0.4609}$	$0.6795\ e^{-j0.4596}$	0.0180	0.0010	0.0090
	2	$0.9855\ e^{j0.0046}$	$0.4538\ e^{-j0.4591}$	$0.4538\ e^{-j0.4591}$	0.0300	0.0068	
	3	$0.9899\ e^{j0.0032}$	$0.1129\ e^{-j0.4605}$	$0.1129\ e^{-j0.4605}$	0.0210	0.0012	
2 (with RPF)	1	$1.0028\ e^{-j0.0009}$	$0.1115\ e^{-j0.4645}$	$0.2203\ e^{j2.6733}$	-0.0058	-0.0003	0.0034
	2	$1.0085\ e^{-j0.0027}$	$0.4435\ e^{j2.6753}$	$0.4435\ e^{j2.6753}$	0.0176	0.0039	
	3	$1.0014\ e^{-j0.0004}$	$0.1116\ e^{-j0.4641}$	$0.1116\ e^{-j0.4641}$	-0.0028	-0.0002	

total losses, while the sum of the total loss sensitivity terms has no constraints. In both cases, the descending-order ranking of the allocated losses and of the total loss sensitivity terms is the same, even without being strictly proportional. These aspects support the conjecture that the allocated losses may have a qualitative meaning linked to the total loss sensitivity terms.

To further investigate the situation, let us present two examples. In Example 1, net power load at node 2 is changed by keeping the same reactive power to active power ratio. Fig. 1 shows the results for net active power load at node 2 changing from −0.35 pu (generation) to 0.15 pu (load). The minimum total losses appear when the net load power is $P_{S2,t} = -0.1$ pu at node 2. The inversion point of the current is at 0 p.u at branch 2, while it is at $P_{S2,t} =$ -0.2 pu at branch 1 (that corresponds to the boundary condition for RPF).

Looking at the total loss sensitivities in a case with *no RPF* (e.g., for net load power $P_{S2,t} =$ 0.1 pu at node 2), the sensitivity $\xi_{2,t}$ is positive: by increasing the net load power, the total losses increase. The total loss sensitivity $\xi_{2,t}$ in RPF conditions (e.g., for shunt node power $P_{S2,t} = -0.35$ pu at node 2) is again positive; however, an increase of the shunt node power, in this case, leads to a reduction of the total losses. How to explain this? The calculation of the sensitivity in Eq. (6) makes use of the shunt node current magnitude, which is always positive, hiding information about the existence of the RPF. Handling this discrepancy requires additional information, i.e., the *sign* of the shunt node power $P_{S2,t}$. In fact, by defining the product $\pi_{2,t} = \text{sign}(\xi_{2,t}) \bullet \text{sign}(P_{S2,t})$, $\mathscr{L}_{\text{tot},t}$ increases when $\pi_{2,t} > 0$, while $\mathscr{L}_{\text{tot},t}$ decreases when $\pi_{2,t} < 0$.

With reference to Fig. 1, the RPF conditions occur for $P_{S2,t} < -0.2$ pu. For $P_{S2,t} < -0.1$ pu, $\xi_{2,t}$ is positive, thus $\pi_{2,t} < 0$ and the total losses decrease. For $P_{S2,t}$ variable from − 0.1 pu to 0, $\xi_{2,t}$ becomes negative, so that $\pi_{2,t} > 0$. For $P_{S2,t} > 0$, $\xi_{2,t}$ is positive and $\pi_{2,t} > 0$, again consistent with the total losses increase.

It has to be noted that the results indicated are valid *only* for the sensitivity calculated at the same node in which the power variation is considered (node 2 in the case shown). To confirm this point, Example 2 is presented, starting from the load power −0.2−j0.05 pu at node 2 and 0.1 +j0.05 pu at node 3, while the load power at node 1 changes with reactive power to active power ratio constant and equal to 0.5. Fig. 2 shows the results for this example. Node 2 contains always a generator and the contribution from node 1 changes from further generation to load. RPF is detected for $P_{S1,t} < 0.1$ pu and the total losses have a minimum for $P_{S1,t} = 0.1$ pu. For $P_{S1,t} < 0$, $\xi_{1,t}$ is positive, thus $\pi_{1,t} < 0$ and the total losses decrease. For $P_{S1,t}$ variable from 0 to 0.1 pu, $\xi_{1,t}$ becomes negative, so that $\pi_{1,t} < 0$, and the total losses still decrease. For $P_{S1,t} >$ 0.1 pu, $\xi_{1,t}$ is positive and $\pi_{1,t} > 0$, consistent with the total losses increase.

The findings shown in the examples indicated above are summarised in Table 3, in which all results are confirmed by the variations in the total losses shown in Fig. 1 and Fig. 2, for the respective examples.

Based on the positive outcomes of these two examples, extensive testing has been carried out on large distribution systems (exemplificative cases are shown in Section 4), leading to the following conceptual result:

Result 1 (*loss sensitivity-based product, LSP*). Considering the quantities $\xi_{k,t}$ and $P_{S2,t}$ determined at node k and time step t, and taking the product:

$$\pi_{k,t} = \text{sign}(\xi_{k,t}) \bullet \text{sign}(P_{S2,t}) \tag{8}$$

the following statements hold:

if $\pi_{k,t} > 0 \quad \rightarrow \quad \mathscr{L}_{\text{tot},t}$ increases

if $\pi_{k,t} < 0 \quad \rightarrow \quad \mathscr{L}_{\text{tot},t}$ decreases

The sensitivity of the total losses used to establish **Result 1** has been determined with respect to the shunt node current magnitude. To explain the validity of the use of the current-based model with respect to other voltage-dependent models (e.g., assigned impedance or assigned power in the classical ZIP model), let us consider a simple two-node system, which is sufficient to identify the relevant aspects.

Starting from the power flow results, looking only at the operating point reached it is not possible to know which voltage-dependent model (e.g., assigned impedance, assigned current, or assigned power) has been used in the calculations. It is then possible to assign any kind of voltage dependence and determine the parameters of the models that correspond to the same operating point. In particular, for a two-node system there are analytical expressions of the line current for different voltage-dependent representations of the operating points, from which it is possible to calculate the sensitivities of the total losses with respect to the model parameters.

For comparing the effect of using different voltage-dependent representations on the sign of the loss sensitivities, a numerical example referring to the two-node system shown in Appendix B is presented. The data considered are $E = 1$ p.u., $R = 0.021$ p.u., and $X = 0.0034$ p.u. (the same impedance of the lines considered in Section 3.1), changing the power values with Q/P ratio equal to 0.5.

Fig. 3 shows the derivatives of the total losses with respect to the parameters of the three models (current magnitude, resistance, and active power) for different values of the active power chosen in such a way to have acceptable voltages (within the range from 0.95 to 1.05 p.u.) at the ending side of the line. The important point referring to the scope of this paper is the sign of the derivatives. The loss derivative with respect to the active power is positive for positive active power and negative for negative active power. This is consistent with the fact that a positive variation in the active power produces more losses when the initial active power is positive and less losses when the initial active power is negative. The loss derivative with respect to the resistance has opposite signs, as the resistance has to be reduced to obtain higher active power.

The loss derivative with respect to the current magnitude is always positive in two-node system analysed. As such, to make the results consistent with the active power variations starting from negative values

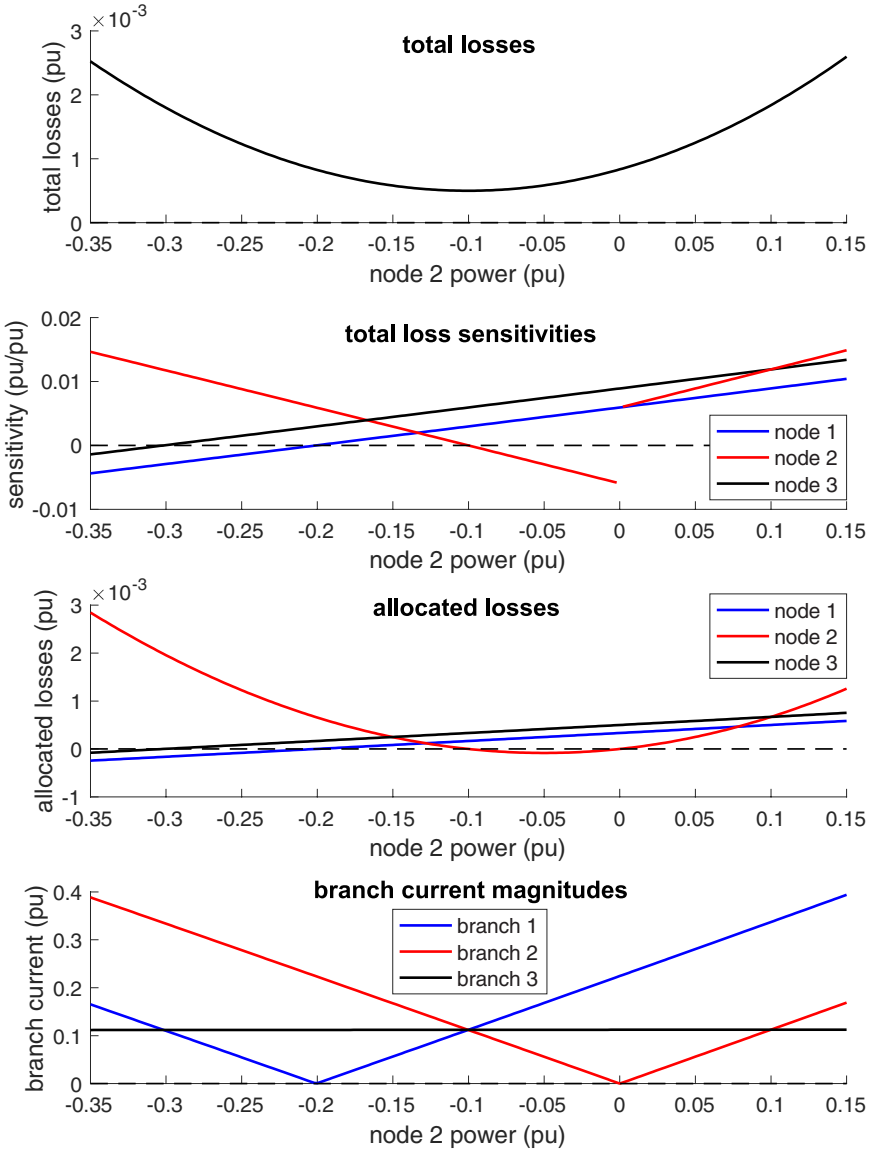

Fig. 1. Examples with changing the shunt node active power at node 2, with $P_{S1} = P_{S3} = 0.1$ pu (base power 100 kVA). Nodes and branches refer to Fig. A1 in Appendix A.

(i.e., from RPF conditions), the loss sensitivity with respect to the current magnitude has to be multiplied by the sign of the active power. This justifies the inclusion of the sign of the active power in **Result 1** of the proposed approach.

The advantage of the proposed approach, as it can already be seen from the equations indicated in Appendix B, is the calculation of the loss derivative with respect to the current magnitude in a simple analytical form. This simplicity remains in the analytical forms for general radial distribution systems provided in Eq. (6) for balanced systems and Eq. (7) for unbalanced systems.

3.2. *Relations between the allocated losses and the total loss sensitivities – balanced system*

Fig. 1 and Fig. 2 show that the sign of the total loss sensitivities with respect to the current magnitude at node k is always equal to the sign of the losses allocated to node k, for any time step $t = 1, \ldots, T$ in every condition (including RPF). It is then possible to replace $\text{sign}(\xi_{k,t})$ in (8) with $\text{sign}(\lambda_{k,t})$. By replacing $\pi_{2,t}$ in Table 3 with the product $\zeta_{k,t} = \text{sign}(\lambda_{k,t}) \bullet \text{sign}(P_{Sk,t})$, the results are indicated in Table 4. The total losses increase or reduction is *exactly the same* in the two tables.

On these bases, a new result is formulated as follows.

Result 2 (*allocated losses-based product, ALP*). Considering the quantities $\lambda_{k,t}$ and $P_{Sk,t}$ determined at node k and time step t, and taking the product:

$$\zeta_{k,t} = \text{sign}(\lambda_{k,t}) \bullet \text{sign}(P_{Sk,t}) \tag{9}$$

the following statements hold:

if $\zeta_{k,t} > 0 \quad \rightarrow \quad \mathscr{L}_{\text{tot},t}$ increases

if $\zeta_{k,t} < 0 \quad \rightarrow \quad \mathscr{L}_{\text{tot},t}$ decreases

Based on the above results, the conceptual insights offered by **Result 1** find their corresponding practical outcomes in **Result 2**. Comparing **Result 2** with **Result 1**, it is interesting to note that **Result 2** offers some major advantages over **Result 1**, as:

a) There is no need for computing the sensitivity terms. This is also useful because, as shown in Fig. 1 and Fig. 2, the sensitivity has a discontinuity when the net load power changes from negative to positive values, while the allocated losses have no discontinuity with the change of the shunt node power.

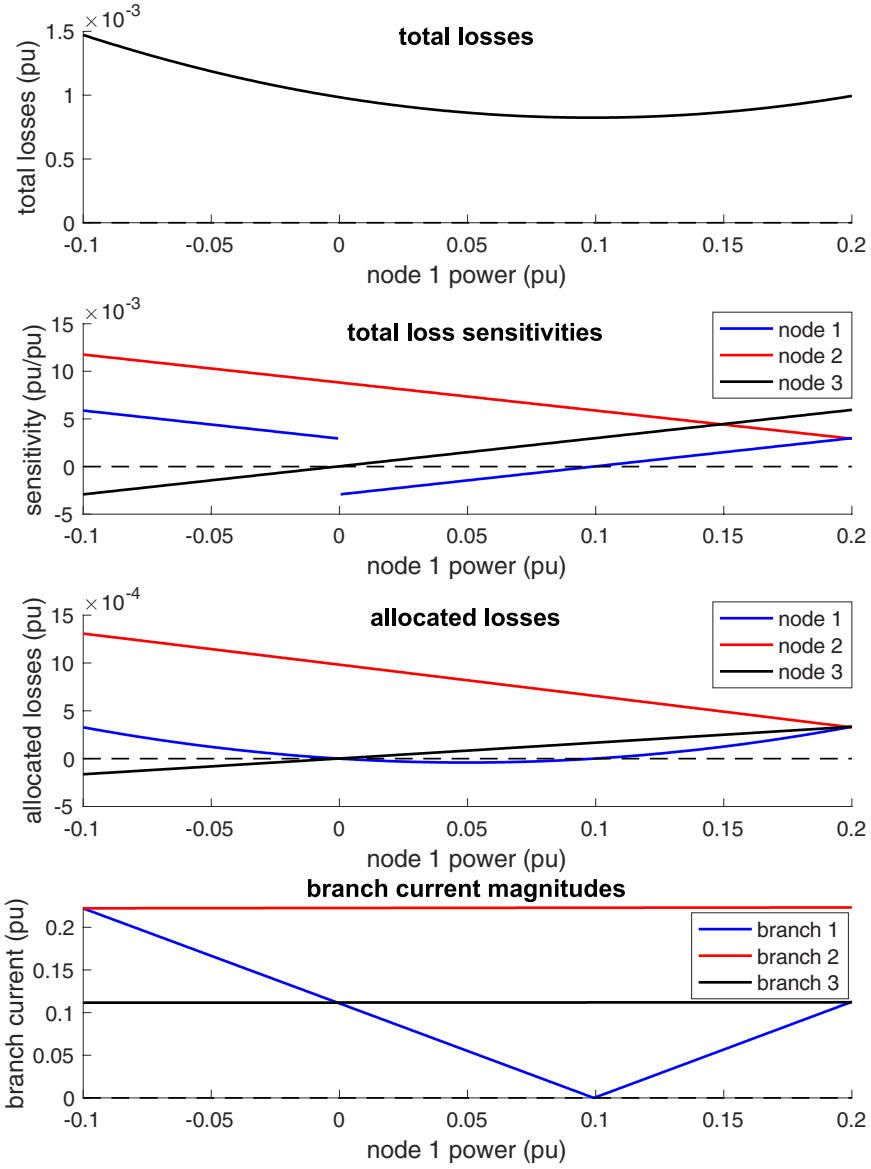

Fig. 2. Examples with changing the shunt node active power at node 1, with P_{S2} = -0.2-j0.05 pu and P_{S3} = 0.1+j0.05 pu (base power 100 kVA). Nodes and branches refer to Fig. A1 in Appendix 1.

Table 3
Results for the two examples with net load power increase.

Example 1					
$P_{S2,t}$ range (pu)	$\xi_{2,t}$	$P_{S2,t}$	$\pi_{2,t}$	total losses	confirmed
< -0.2	> 0	< 0	< 0	decrease	yes
-0.2 ÷ −0.1	> 0	< 0	< 0	decrease	yes
-0.1 ÷ 0	< 0	< 0	> 0	increase	yes
> 0	> 0	> 0	> 0	increase	yes
Example 2					
$P_{S1,t}$ range (pu)	$\xi_{1,t}$	$P_{S1,t}$	$\pi_{1,t}$	total losses	confirmed
< 0	> 0	< 0	< 0	decrease	yes
0 ÷ 0.1	< 0	> 0	< 0	decrease	yes
> 0.1	> 0	> 0	> 0	increase	yes

b) The allocated losses are easy to compute from the power flow results, keeping the important meaning that their sum is equal to the total losses. It is worth noting that all the entries needed for the calculation of the allocated losses are already available from the power flow solution.

3.3. *Relations between the allocated losses and the total loss sensitivities – unbalanced system*

In unbalanced systems, there is one more variant with respect to the cases shown for the balanced system, namely, the different behaviour of the phases. In particular, RPF could appear on one of two phases only. After extensive testing on various unbalanced networks (an example is reported in Section 4.2), the same results obtained for the balanced system have been confirmed on a single-phase basis, using the allocated losses from Eq. (3) and the sensitivities from Eq. (7).

The version of **Result 1** for unbalanced systems is then formally represented as:

Result 1 (*loss sensitivity-based product, LSP*). Considering the quantities $\xi_{k,p,t}$ and $P_{Sk,p,t}$ determined at phase p of node k and time step t, and taking the product:

$$\pi_{k,p,t} = \text{sign}(\xi_{k,p,t}) \bullet \text{sign}(P_{Sk,p,t}) \tag{10}$$

the following statements hold:

if $\pi_{k,p,t} > 0 \quad \rightarrow \quad \mathscr{L}_{\text{tot},t}$ increases

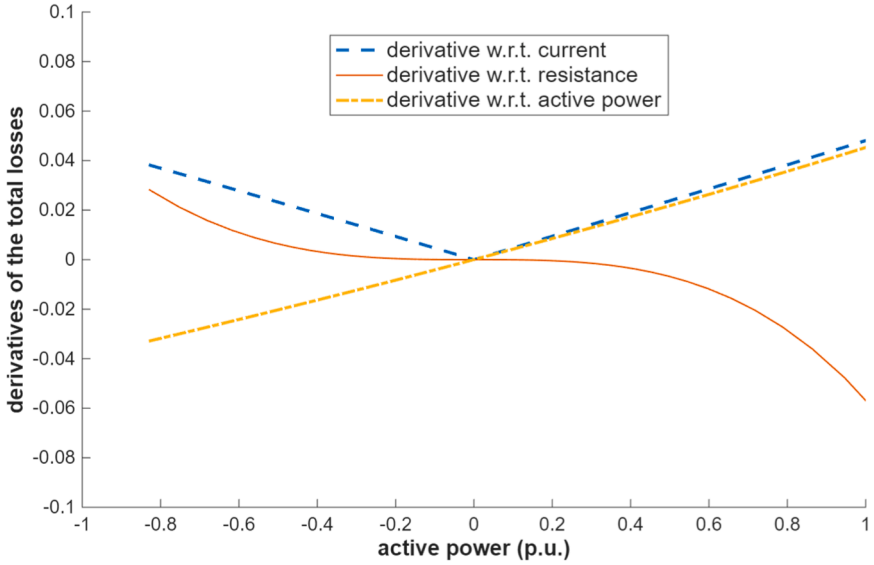

Fig. 3. Derivatives of the total losses with respect to the parameters of current magnitude, resistance, and active power models (base power 100 kVA).

Table 4
Results of the two examples with allocated losses and net power variation.

Example 1					
$P_{S2,t}$ range (pu)	$\lambda_{2,t}$	$P_{S2,t}$	$\zeta_{2,t}$	total losses	Confirmed
$<$ -0.2	>0	<0	<0	decrease	Yes
-0.2 $\div$ -0.1	>0	<0	<0	decrease	Yes
-0.1 $\div$ 0	<0	<0	>0	increase	Yes
>0	>0	>0	>0	increase	Yes
Example 2					
$P_{S1,t}$ range (pu)	$\lambda_{1,t}$	$P_{S1,t}$	$\zeta_{1,t}$	total losses	Confirmed
<0	>0	<0	<0	decrease	Yes
0 $\div$ 0.1	<0	>0	<0	decrease	Yes
>0.1	>0	>0	>0	increase	Yes

if $\pi_{k,p,t} < 0 \quad \rightarrow \quad \mathscr{L}_{\text{tot},t}$ decreases

with the same limitations indicated for the balanced case, regarding the assumptions needed for the sensitivity calculations.

The version of **Result 2** for unbalanced systems is formally represented as follows:

Result 2 (*allocated losses-based product, ALP*). Considering the quantities $\lambda_{k,p,t}$ and $P_{Sk,p,t}$ determined at phase p of node k and time step t, and taking the product:

$$\zeta_{k,p,t} = \text{sign}\left(\lambda_{k,p,t}\right) \bullet \text{sign}\left(P_{Sk,p,t}\right) \tag{11}$$

the following statements hold:

if $\zeta_{k,p,t} > 0 \quad \rightarrow \quad \mathscr{L}_{\text{tot},t}$ increases

if $\zeta_{k,p,t} < 0 \quad \rightarrow \quad \mathscr{L}_{\text{tot},t}$ decreases

Result 2 with the *ALP* formulation is then the main novel fundamental contribution of this paper, for balanced and unbalanced radial distribution systems.

Fig. 4 presents the flow-chart of the calculation of the products *LSP* and *ALP* for a distribution system for which the loads and generations are provided as inputs for the time steps of analysis $t = 1, \ldots, T$. At each time step, after solving the power flow, both the sensitivities of the total losses with respect to the current magnitude and the allocated losses are computed from the analytical expressions for balanced or unbalanced systems. The products *LSP* and *ALP* are calculated by using the sign of the sensitivities and the allocated losses, respectively. In computational terms, after the power flow solution, the calculations that provide the *LSP* or *ALP* are computationally almost inexpensive, as only analytical expressions are used.[4] The results are used to identify the nodes at which a small change of net node power can lead to an increase or reduction of the total losses. In the figure, the parts referring to the calculation of the *LSP* are marked with dashed lines because, after having shown the conceptual relations between total loss sensitivities and allocated losses, the suggested solution is the one with the *ALP* calculation.

For distribution systems, the Z-bus loss allocation method [36] (in its version that does not consider the loss allocation to the slack node) is a resistance-based loss allocation method that provides the same results of the BCDLA method. As such, the outcomes of the *ALP* calculations would be the same also by using the Z-bus loss allocation method to determine the allocated losses. In the proposed approach, the allocated losses and the expression of the loss sensitivity with respect to the current magnitude are determined by using the line resistance (or the 3×3 resistance matrix for unbalanced systems) without the need for constructing the bus impedance matrix of the system, which is not requested in the solution of the backward/forward sweep algorithm.

The approach introduced and discussed in this paper refers to radial distribution systems, based on the power flow results. The same calculations can be carried out in loop or weakly meshed distribution systems, applying the effective methodology for power flow solution formulated in the literature [51]. This methodology defines breakpoints for each loop to form a radial network, then executes a compensation method

[4] For a quantitative assessment of the computation times, tests have been carried out a personal computer with processor 13th Gen Intel(R) Core(TM) i7–1355U (1.70 GHz) with 16 GB RAM. For the balanced system considered in Section 4.1, the mean computation time for solving one power flow is about 20 ms. For the computation of *ALP* and *LSP* from the analytical formulations, due to the very fast times, the computation time has been determined by modifying on purpose the code to repeat the same calculation 1000 times, then dividing the outcome by 1000. The resulting mean computation time is about 20 μs for *ALP* and 0.7 μs for *LSP*.

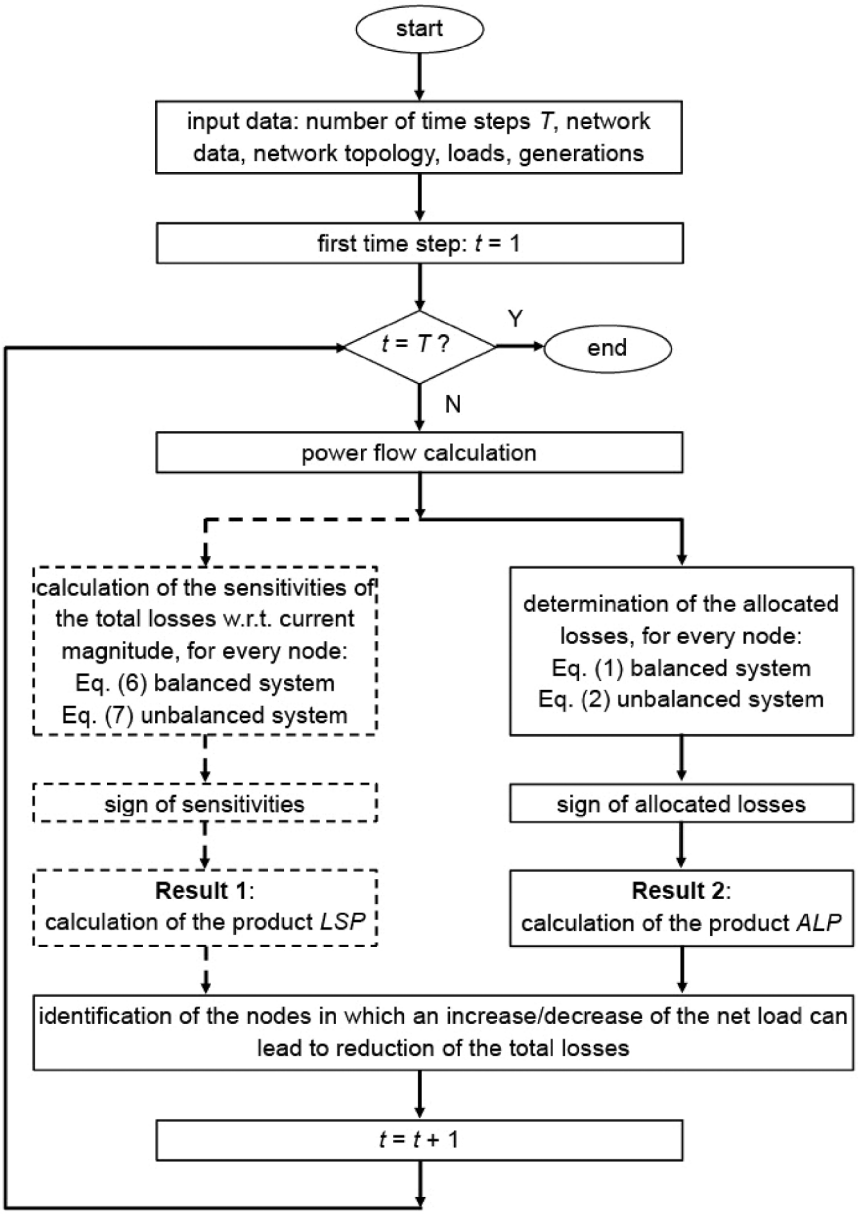

Fig. 4. Flow-chart for the calculation of *LSP* and *ALP*.

based on injecting a current in the breakpoints and solving the radial network in an iterative way until the voltage magnitudes at the terminals of the breakpoint nodes are lower than the specified tolerance. In this way, the solution obtained by solving radial networks is the same that would be obtained by solving the meshed network with an appropriate solver. Hence, *LSP* and *ALP* can be calculated starting from this solution.

4. Application cases

4.1. Balanced system data and results

The Medium Voltage distribution system considered is supplied by a 150 kV / 20 kV transformer and serves a rural area [53]. The radial network is shown in Fig. 5, with 102 nodes that belong to seven feeders (denoted as F1-F7). The network contains five PV generators located at nodes 9 (1 MW peak), 31 (2 MW peak), 33 (3 MW peak), 41 (1 MW peak), and 48 (1 MW peak), with the same reference active power profile (normalised, to be multiplied by the reference power of each PV generator to obtain the PV generation at each node) and null reactive power. The base power is 1 MVA. The power flow is executed by considering the tolerance equal to 10^{-5} on the relative voltage variation between two successive iterations for the stop criterion.

The net load power changes during time at each node, following specific daily load patterns, with regular time steps of a quarter of hour. Fig. 6 shows the average active power and reactive power injected into the grid at each quarter of hour, indicated in per unit (pu) values. RPF occurs in the quarters of hour from 46 to 55.

Fig. 7 shows the heatmap that corresponds to the values of $\zeta_{k,t}$ found from the power flow solutions for the $k = 1, \ldots, K$ nodes and $t = 1, \ldots, T$ time steps. Most values are $+1$ (i.e., the total losses increase by increasing the net load power in the node). Some values are null, corresponding to null or negligible loads (i.e., less than 1 W). The cases with values equal to -1 correspond to the reduction of the total losses by increasing the net load power in the node. In Fig. 7, for better legibility the 20 quarters of hour at the beginning of the day and the 20 quarters of hour at the end of the day are not represented. In these quarters of hour, the values at every node are respectively equal to the values of the first

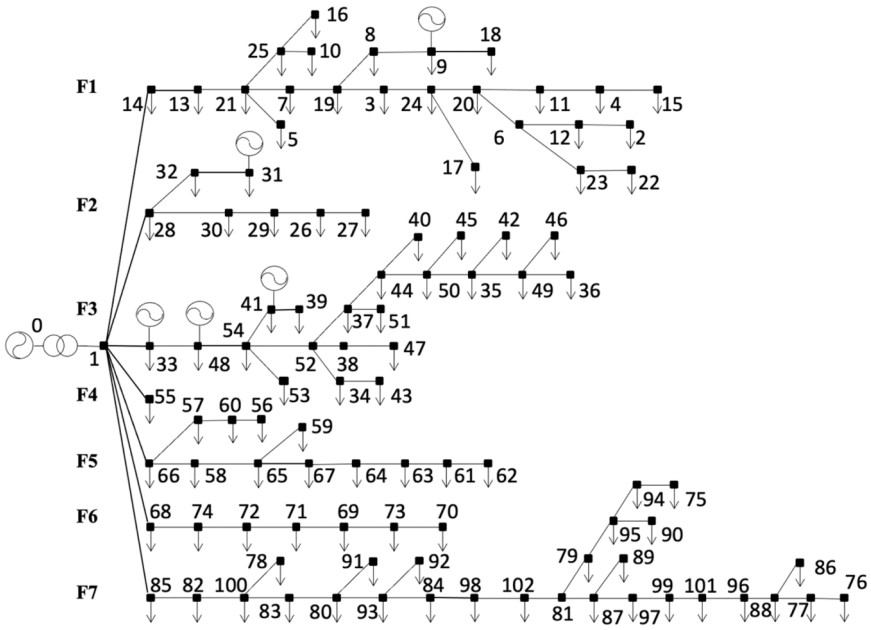

Fig. 5. Balanced three-phase system [53]. The PV systems located in the nodes 9, 31, 33, 41, and 48 are represented as generators.

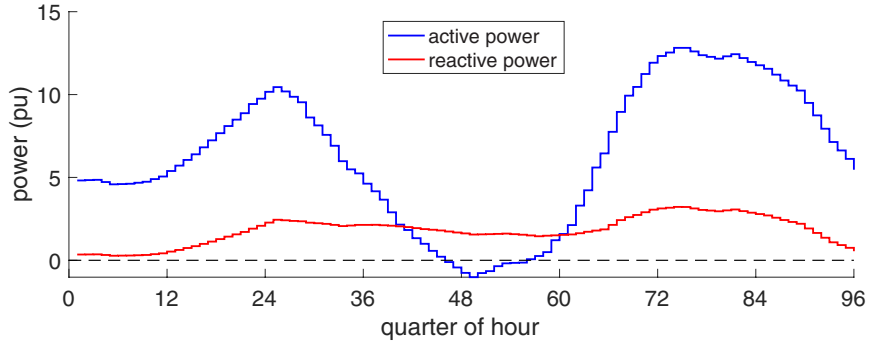

Fig. 6. Active and reactive power injected into the distribution system from the slack node (base power 1 MVA).

and last quarters of hour shown in the figure. The results shown in the heatmap have been confirmed by executing a test with net complex power increased by 0.1% in each node with non-null load (with positive increase also in the nodes with negative loads), one at a time, computing each time the total losses that have been compared with the total losses in the initial power flow solution. The small perturbations applied to the initial load to compute the total loss sensitivities have been chosen to balance the need of imposing small variation to the operating point for maintaining the validity of the linear approximation with the need of obtaining non-negligible changes of the values used in the calculation of the sensitivities.

In particular, negative values of $\zeta_{k,t}$ appear in the central period of the day in the nodes 33–54, belonging to the feeder F3, in which there is a concentration of PV generation. Moreover, negative $\zeta_{k,t}$ appears at node 55 (feeder F4) in RPF conditions, meaning that the increase of the net load power at node 55 would be beneficial to reduce the total losses by mitigating RPF. The same situation appears in the nodes 8, 9, 18 and 19 in Feeder F1, close to the PV generation at node 9, and at nodes 31 and 32 in feeder F2 (close to the PV generation at node 32), with the addition of node 30 in some cases with RPF conditions (connected to node 28 that has no load and as such has null values of $\zeta_{k,t}$ during the day).

Fig. 8 shows a representative result, considering node $k = 48$ (with PV generation), belonging to Feeder F3, in which there are many aspects to discuss. The first plot of Fig. 8 shows the sensitivity $\xi_{k,t}$. The next five plots refer to the allocated losses and net load active power, with the corresponding signs, leading to the product $\zeta_{k,t}$ of **Result 2**, equal to the product $\pi_{k,t}$ of **Result 1**. The last plot shows the variation of the total losses after the small net load additions at each time step, whose sign confirms the correctness of **Result 1** and **Result 2** in identifying the conditions that lead to the total network losses increase (positive sign) or decrease (negative sign). These results refer to the total losses of the whole network, not only of the feeder F3 in which node 48 is located.

4.2. *Unbalanced system data and results*

The unbalanced system considered is the IEEE European Low Voltage Test Feeder [54]. The system has 905 nodes plus the slack node, contains 55 single-phase loads, and is supplied at 416 V phase-to-phase. The evolutions in time of the loads are taken from the available system data, with average power values at each quarter of hour. Ten single-phase PV generators with rated power 4 kW each have been added to the ten nodes with the highest rated load (phase a of nodes 348 and 562, phase b of nodes 248, 405, 754 and 885, and phase c of nodes 263, 326, 555 and 618), with the same evolution in time of the PV power generation for a clear sky day used for all PV generators.

The power flow is executed by considering the tolerance equal to 10^{-5} on the relative voltage variation between two successive iterations

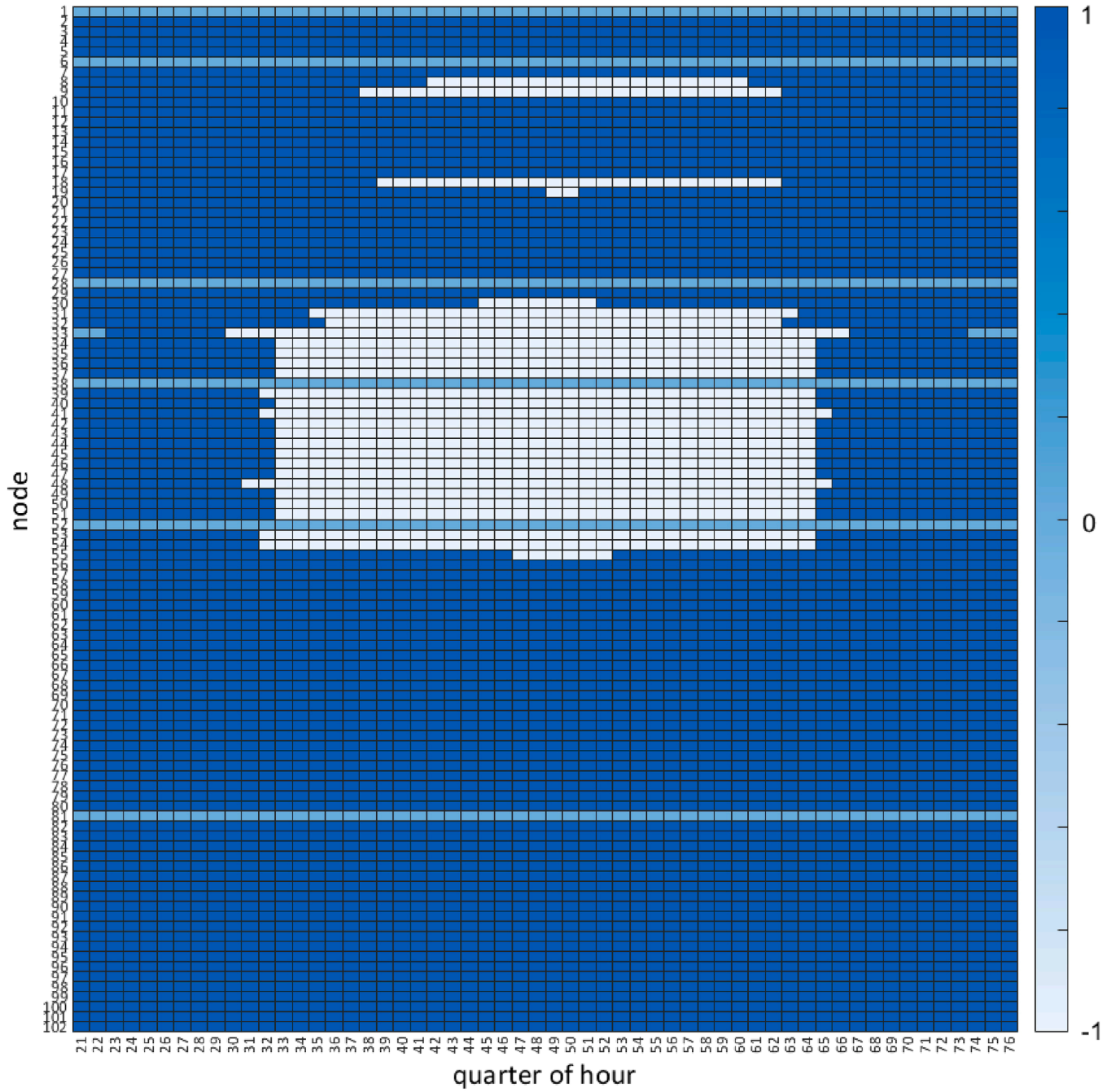

Fig. 7. Heatmap with the term $\zeta_{k,t}$ for the $k = 1, \ldots, K$ nodes and $t = 1, \ldots, T$ time steps. The relevant values represented with different colours are -1, 0, and $+1$.

for the stop criterion. The analysis carried out on 96 time steps (quarters of hour) for one day provided the same products $\pi_{k,p,t}$ and $\zeta_{k,p,t}$ for **Result 1** and **Result 2** in all the cases tested. Fig. 9 shows the heatmaps of the product $\zeta_{k,p,t}$ for the three phases obtained at time steps $t = 1, \ldots, T$, considering the variability of the operating conditions during time. In Fig. 9(a, b and c), for better legibility the 10 quarters of hour at the beginning of the day and the 10 quarters of hour at the end of the day are not represented, the values at every node being respectively equal to the values of the first and last quarters of hour shown in the figure. The situation of the three phases of the same node is different because of the different composition of the loads and generations in each phase. In particular, the testing confirmed that the sign of the sensitivities determined from (7) and the sign of the allocated losses calculated from (3) are equal at each time step for each node and phase. To exemplify, let us take two cases, at phase b of node #177 (load only) and phase c of node #326 (load and PV). Fig. 10 shows the sensitivities and allocated losses on the top graph, and their (equal) sign on the bottom graph.

Finally, it is confirmed that in all nodes, phases and time steps, the signs indicated in the heatmaps correspond to the sign of the total loss variation. For this purpose, the difference between the total losses obtained after the addition of 0.1% of the load to the base case load and the total losses in the initial power flow solution has been computed at every single node, phase and time step. Fig. 11 shows that the sign of the total loss variation is equal to the sign seen in the corresponding heatmap (Fig. 9) for phase b of node 177 and phase c of node 326.

The typical time steps used for interval metering in distribution systems are 15 min, 30 min, and one hour. The examples shown above considered a quarter of hour as the time step. The results change if a different time step is used. In particular, less resolution (i.e., with a longer time step) leads to smoother power patterns, losing information

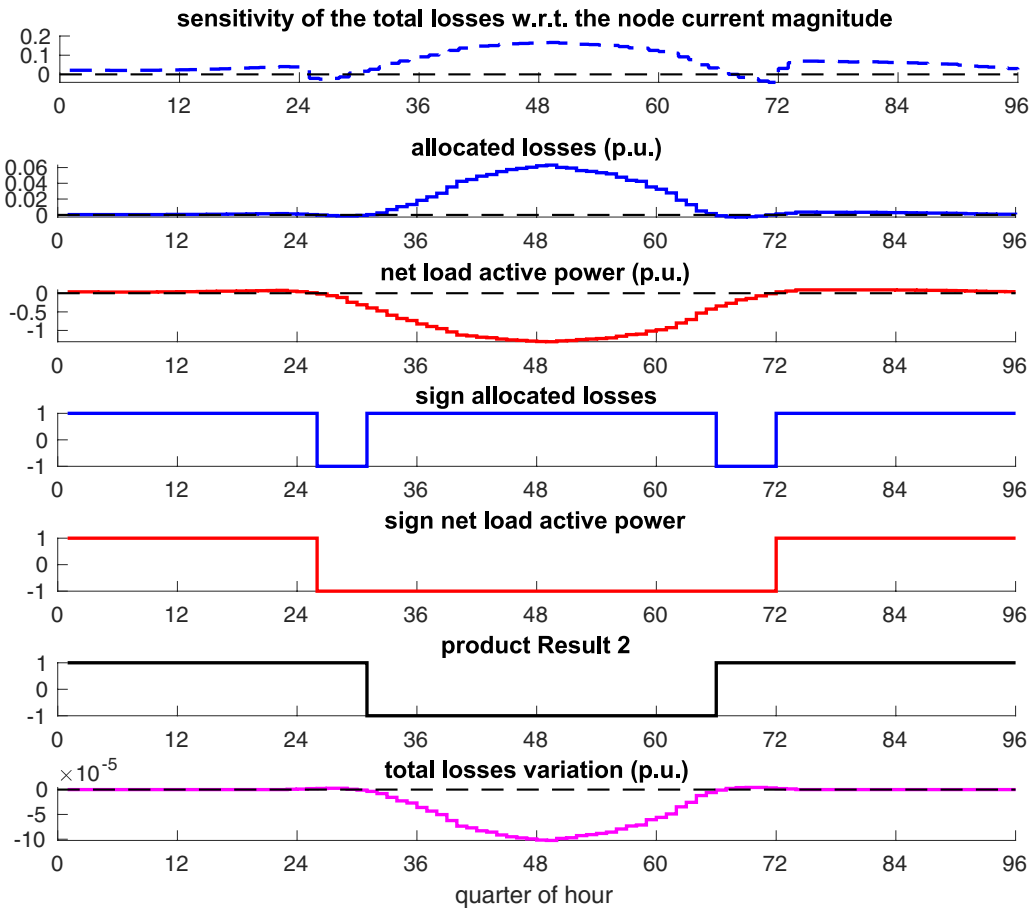

Fig. 8. Results of the representative example on node 48 (base power 1 MVA).

about the variability of the patterns during time. With different fluctuations in demand and generation, the net load power could change sign, but if these fluctuations are not detected because of the averaging process that forms the data for the longer time step, the ALP values resulting from the analysis at each node are less variable with respect to the ones found by using shorter time steps. This situation is shown in Fig. 12 for phase c of node #326, in which, compared with Fig. 10b, less changes in the sign of loss sensitivities and allocated losses are detected.

4.3. ALP applications to distribution system operation and planning cases

Based on the link identified between the signs of allocated losses and total loss sensitivities, the ALP values indicated in **Result 2** can be applied to any situation presented in the literature that involves the calculation of loss sensitivities with respect to the (net) load, as mentioned in Section 1.1. The applications refer to distribution system operation (at individual time steps, with constant load) and planning (with the possible addition of new components in the system and the analysis of scenarios of evolution of the distribution system).

Two examples are provided below, for cases related to distribution system operation and planning, respectively. In these cases, changes are introduced in the distribution systems, requiring power flow computations in different situations. To keep consistency with the sensitivity link, the changes analysed should be relatively limited in amplitude, and after each change the ALP values are recalculated to check whether any change of sign has occurred.

4.3.1. Operational case – PV power curtailment

In a distribution system, if the installed non-programmable capacity from renewable energy sources is relatively high, it may happen that part of the generation from renewable energy has to be curtailed to avoid the violation of distribution system constraints. PV generation curtailment could be needed especially during bright days when there is high PV power injection in the grid. An exemplificative case is constructed on the IEEE European Low Voltage Test Feeder [54]. Since the cases analysed in Section 4.2 have no constraint violation, the PV power in the initial network is increased at individual locations, as follows: PV power is increased 10 times for 8 out of the 10 PV systems (the ones connected to phase b and phase c), as indicated in Section 4.2, to create a situation where violations (due to over-voltages) result from the power flow calculations. Starting from this situation, the ALP values have been calculated at quarter of hour #50 from the power flow results at each node with PV systems, resulting in 2 nodes with $+1$ value (node #348 and node #562) and the other 8 nodes with -1 value.

PV power curtailment has been applied in different ways:

1) to all PV nodes, with curtailment proportional to the PV power, until no violations have been reached, resulting in the PV power curtailment of 67.2 kW.
2) only to the PV nodes with ALP equal to -1, with progressive 1% curtailment proportional to the PV power for these nodes only, until no violations have been reached, resulting in PV power curtailment of 64.8 kW.

Comparing the results, the application of the ALP values to select the PV systems subject to PV power curtailment for avoiding constraint violations has resulted in lower curtailment, showing the benefit of introducing a PV system selection criterion based on the proposed findings. This result has been confirmed for other quarters of hour, as shown in Fig. 13 for the quarters of hour in which there are violations

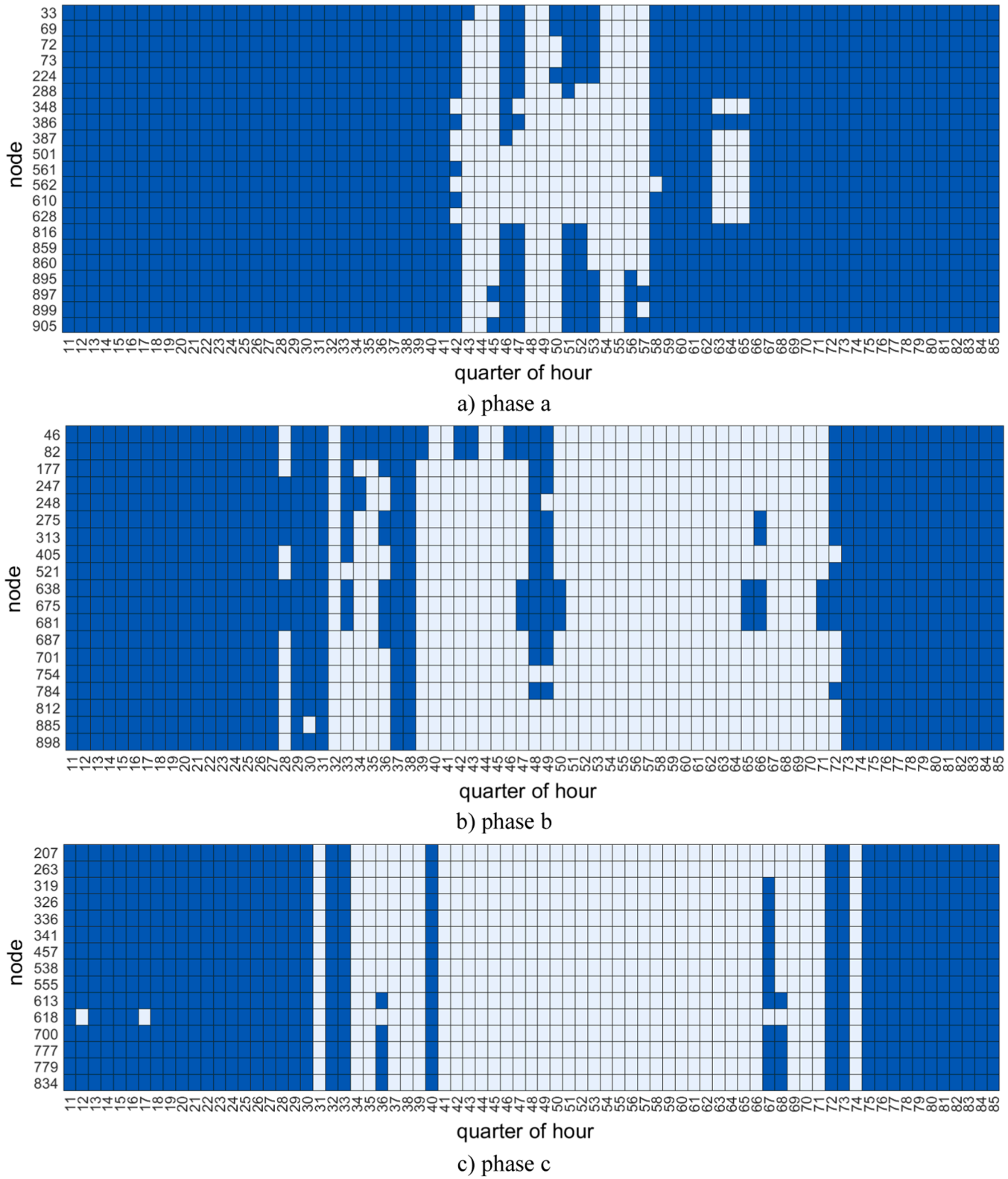

Fig. 9. Heatmap representation of the product $\zeta_{k,p,t}$ for the $k = 1, \ldots, K$ nodes and $t = 1, \ldots, 96$ time steps in the unbalanced case. Dark colour is used for the value $+1$, and light colour for the value -1.

that need PV power curtailment to be removed.

4.3.2. *Planning scenario-related case – PV power addition*

A common analysis for planning purposes is the addition of new PV systems to a selected set of system nodes. The addition can be done in different ways, creating suitable scenarios. The base scenario considered in the example shown here is the addition of the same PV power to all the PV nodes in which there is no PV system in place. This addition considers a scalar factor that drives the PV power increase until a violation occurs in the distribution system. The calculations are carried

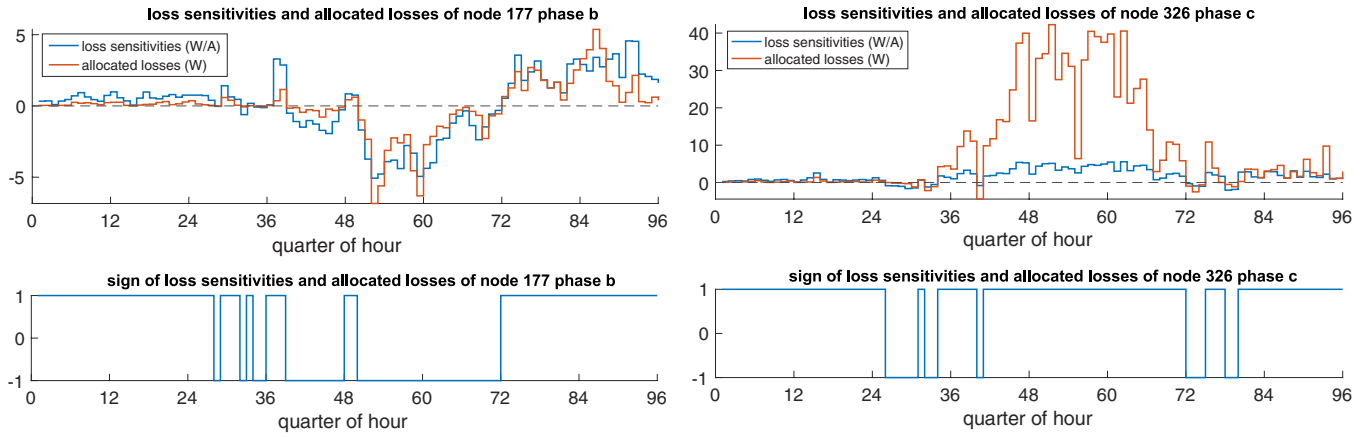

a) phase b of node 177 b) phase c of node 326

Fig. 10. Signs and values of the sensitivities of the total losses with respect to the current magnitude variation and of the allocated losses in different phases of the selected nodes, for $t = 1, \ldots, 96$ time steps.

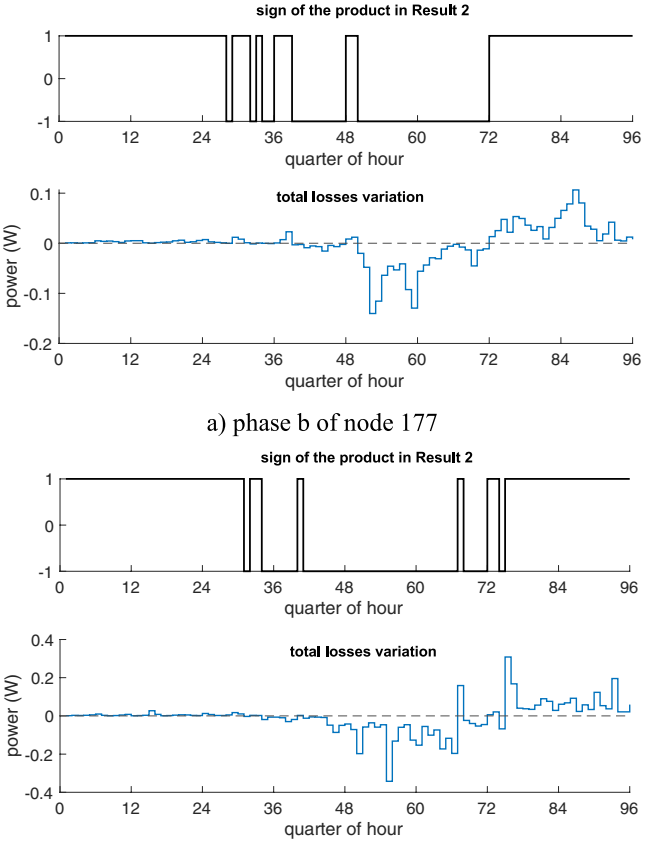

a) phase b of node 177

b) phase c of node 326

Fig. 11. Comparison between $\zeta_{k,p,t}$ in **Result 2** and the total loss variation for the unbalanced case in selected nodes and phases, for $t = 1, \ldots, 96$ time steps.

out for the balanced system,[5] starting with the solutions already presented in Section 4.1, which refer to clear sky conditions. The period considered includes the central hours of the day, at the quarters of hour

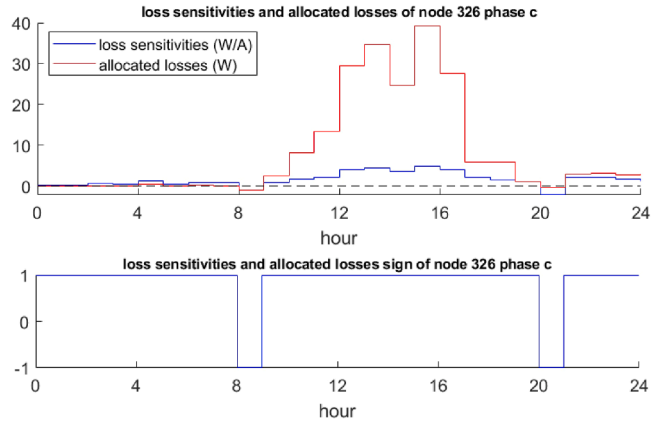

Fig. 12. Signs and values of the sensitivities of the total losses with respect to the current magnitude variation and of the allocated losses at phase c of node #326, for hourly time steps.

from #40 to #60. Based on these results, the PV power addition in this scenario cannot be higher than the minimum value of the maximum PV additions that occur at each time step without violating the constraints.[6]

In the scenario indicated above, there is no consideration on the distribution system losses. A novel methodological approach is presented here, in which the selection of the PV systems in which the PV power is added is driven by the calculation of the ALP values. This approach proposes a new way to create a scenario that can be used as a benchmark for determining the possible addition of PV systems to the distribution network nodes.

Starting from the same initial solution considered in the previous strategy, the addition of PV power is enabled only for a selected set of nodes with ALP $= +1$ that indicates an expected reduction in the total network losses. This new scenario has been implemented by assuming small progressive increases of the PV power to be installed (i.e., 1 kW at each node) to keep consistency with the link between ALP and loss sensitivity originally explained in this paper. The ALP values are recalculated from the power flow results after each PV power increase.

The results obtained are first illustrated with reference to an individual time step (i.e., time step #50). The total PV generation increase is

[5] The same approach can be used in the unbalanced system. However, in the solution presented in this paper, the ALP is always equal to -1 for every node in some time steps, and for these time steps the proposed ALP-based strategy for identifying the locations for adding new PV systems cannot be applied.

[6] The example reported here is limited to a single day. More general evaluations are needed on multiple days to identify the most conservative results for PV power addition.

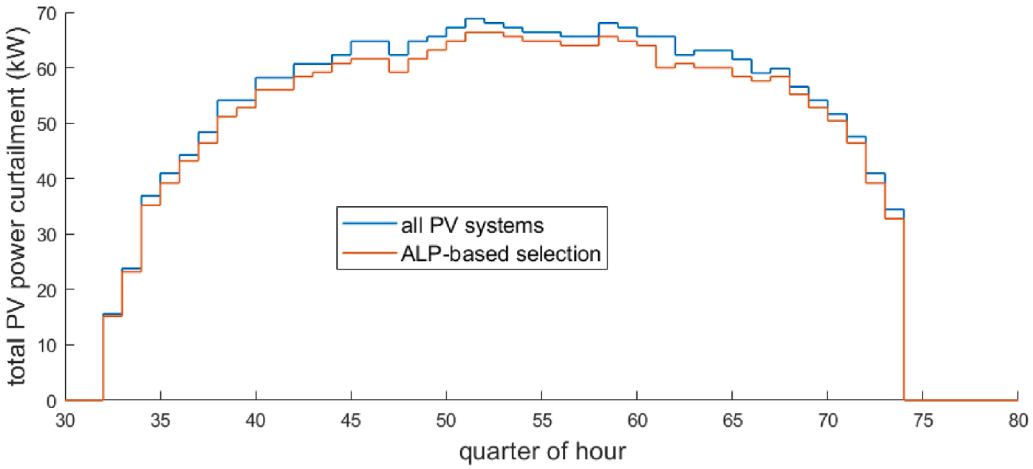

Fig. 13. PV power curtailed in the quarters of hour in the central part of the day.

shown in the blue curve of Fig. 14, until there is a violation in the distribution system, which appears for a total PV power increase of 7.49 pu. In this scenario, the total losses increase.

In Fig. 15a, the ALP values are reported to show that there is no particular regularity when the total PV generation increases. By applying the proposed ALP-driven strategy, the results are shown in the red curve of Fig. 14. The PV generation increase stops when only one PV generator remains with ALP equal to $+1$, for a total PV power increase of 5.70 pu. Note that in these conditions there is no violation. Fig. 15b shows the evolution of the ALP values at each node during the progressive increase of the PV power. When the ALP value at a node passes from -1 to $+1$, the PV power increase at that node is stopped.

The scenarios illustrated above have been executed for the time steps from #40 to #60. The upper plot in Fig. 16 shows the maximum total PV power added at each time step before reaching a constraint violation for the base scenario, together with the corresponding total PV power added in the same time step until a single node remains with ALP $= +1$. The lower plot of Fig. 16 indicates the corresponding total losses. The interesting result is that it is possible to establish a novel strategy of addition of PV power that reduces the total losses for the benefit of the distribution system, resulting (in the example shown) in a significant PV power addition even without reaching the condition of constraint violation. Of course, the installation of new PV systems depends on the decisions of the active users connected to the network, so that this strategy could be used to define priorities for the introduction of new PV systems in the network. In any case, this strategy is useful as a benchmark to establish potential advantages for the distribution systems.

If the potential locations in which the active users intend to install their PV systems are known, the analysis carried out can be applied starting from these locations and selecting the locations for the PV system addition by using the ALP-driven strategy.

5. Concluding remarks

This paper has introduced some original and fundamental findings in the analysis of three-phase balanced and unbalanced radial distribution systems. After the definition of a novel formulation to calculate the sensitivities of the total losses with respect to the shunt node current magnitude for balanced and unbalanced systems, the attention has been focused on the interpretation of the relation between these sensitivities and the losses allocated to the system nodes in various operating conditions, including cases with reverse power flow.

Two new fundamental results have been presented:

1) The sign of the sensitivities of the total losses with respect to the shunt node current magnitude is equal to the sign of the losses allocated to the same node by the methods BCDLA (for balanced systems) and RCLP (for unbalanced systems). The relation between the sign of allocated losses and the sign of total loss sensitivities, although not formally proven analytically, has been extensively validated through numerical testing on both balanced and unbalanced radial distribution systems of varying size and complexity under the assumptions considered (small shunt net power variations and fixed current angles).

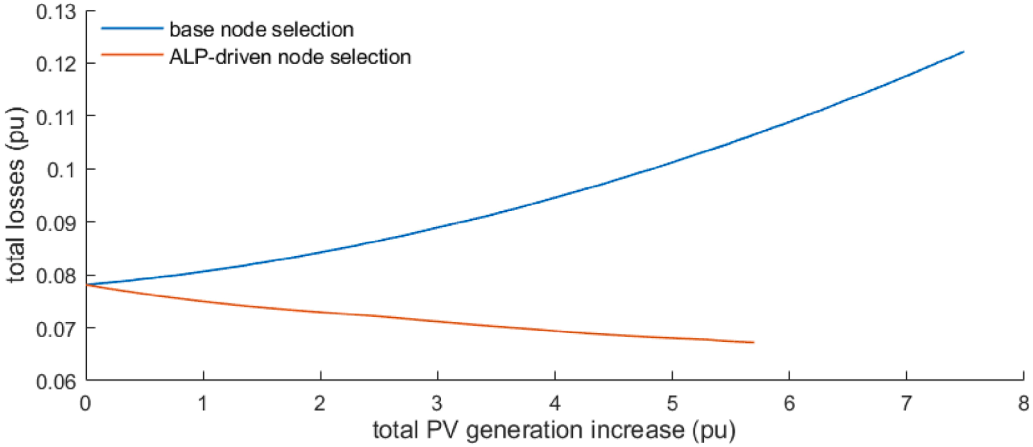

Fig. 14. Comparison between PV power increase scenarios with new PV systems installed at time step $t = 50$ (base power 1 MVA).

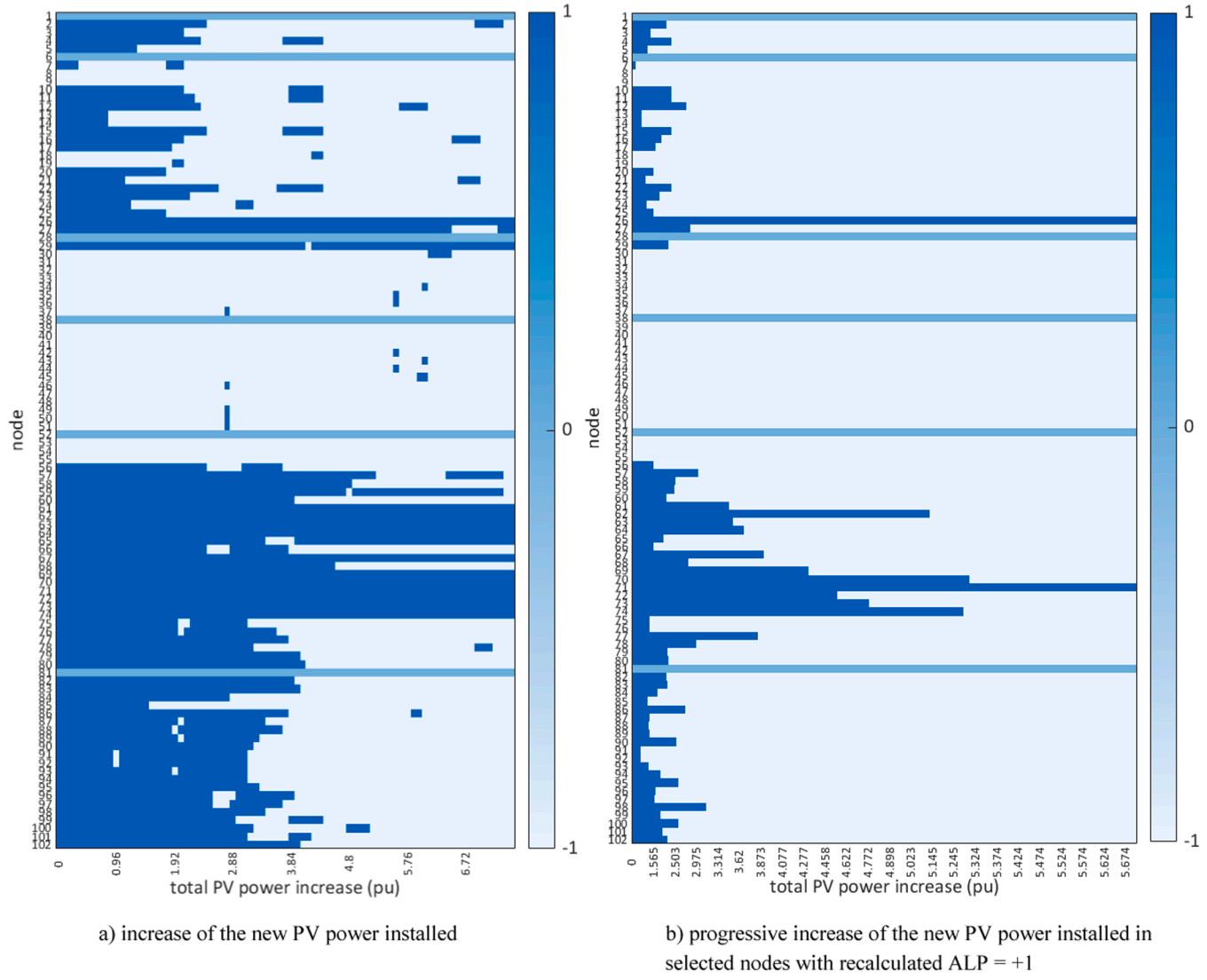

Fig. 15. Scenario at time step $t = 50$. The relevant values represented with different colours are -1, 0, and $+1$. Base power: 1 MVA.

2) The product between the sign of the allocated losses and the sign of the shunt node power, at each node, provides consistent information on the increase or reduction of the total losses in case of a small power variation applied to the corresponding node. For a slight shunt node power increase, the negative sign of the product corresponds to the total loss reduction, while the positive sign means the increase of total losses. The same indication is provided by the product of loss sensitivities times the sign of the shunt node power. However, the latter case has lower computational efficiency, because of the assumptions needed in the loss sensitivity calculations and the discontinuity of the loss sensitivity in case of negligible (close to zero) shunt node power.

The ALP product indicated in **Result 2** of the paper is then proposed as the appropriate indicator, based on the power flow solutions computed during time, to determine whether there is an excess or a lack of shunt node power in each node.

The conceptual link between the result and sensitivity concepts indicates that the result is valid only for small variations of the shunt node power. Large variations have been analysed as a sequence of smaller variations, by calculating the power flow solution and the ALP values after each variation.

The concepts formulated in the paper refer to radial distribution systems, for which the analytical expressions of the loss sensitivities have been introduced. However, these results are also valid for non-radial systems (e.g., loop structures or weakly meshed systems) for which the power flow is solved by using the backward/forward sweep method starting from the identification of breakpoints to obtain radial systems, using the compensation procedure until all voltages between the nodes corresponding to the breakpoints are lower than the predefined tolerance. At this point, the power flow solution of the radial networks is equivalent to the solution of the loop or weakly-meshed system that could be obtained with other solvers. The proposed calculation of the sensitivities and allocated losses can be applied to the radial networks obtained at the convergence of the compensation procedure. Hence, the outcomes of the proposed approach are valid for radial and weakly-meshed networks, covering the typical network distribution system structures.

The results found in this paper are useful for both distribution system operation and planning. The applications presented have highlighted some cases in which the novel possibility of selecting the network nodes and phases to introduce variations in the PV generation has provided tangible benefits. On the operation side, lower PV power curtailment has been obtained by selecting the nodes in which curtailment can be applied from the ALP values, with respect to the proportional curtailment in all PV systems. The proposed strategy can then be seen as a

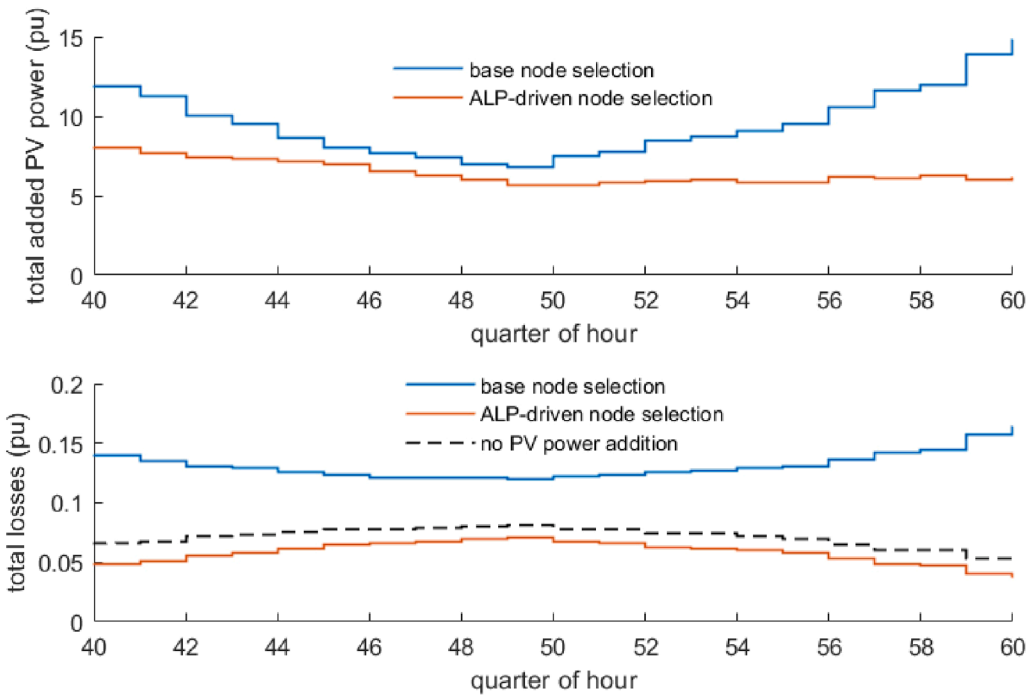

Fig. 16. Total added PV power and total losses in the two scenarios considered for the quarters of hour in the central part of the day (base power 1 MVA).

viable new alternative to existing strategies. More generally, for DER curtailment, nodes with negative ALP values indicate where small reductions in generation can reduce total losses, enabling more targeted and efficient curtailment strategies. In the context of demand response, ALP can guide the selection of nodes where incremental load adjustments lead to beneficial effects on the reduction of network losses.

On the planning side, a novel strategy for creating a benchmark to drive the installation of new PV systems has been formulated, which allows considerable PV power increase, enabling in the meanwhile a reduction of the total losses. This scenario can be used as a viable benchmark to support the decisions about positioning and sizing local resources based on the simulation results of the distribution system operation during time. For hosting capacity studies, evaluating ALP across all nodes provides insights into locations where additional DERs can be integrated with reduced impact on the total losses. These applications highlight the potential of ALP to support operational decision-making and planning in real-world distribution systems.

The proposed contribution has some limitations and openings for future work. The loss allocation and sensitivity analyses provide useful indicators, but they are primarily valid for small variations in shunt node power. For large variations, multiple successive power flow calculations are required, which reduce computational efficiency. In addition, the economic implications of the allocated losses have not been included in this study. Future developments include more comprehensive cost–benefit analysis to support decision-making for DSOs based on the outcomes of the analyses presented in this article.

Moreover, work is in progress to apply the proposed findings to different networks in various operating conditions. Relevant cases consider the application of ALP values to study the temporary addition of mobile generation resources to improve distribution system operation, other ways to curtail PV power based on exported power or fairness principles, and the management of the resources of active users in energy communities.

CRediT authorship contribution statement

Gianfranco Chicco: Writing – original draft, Writing – review & editing, Supervision, Software, Methodology, Conceptualization. **Andrea Mazza:** Writing – original draft, Writing – review & editing, Validation, Software, Formal analysis, Conceptualization. **Soheil Saadatmandi:** Writing – original draft, Writing – review & editing, Software, Investigation, Formal analysis, Data Curation.

Declaration of Competing Interest

The authors declare the following financial interests/personal relationships which may be considered as potential competing interests: Soheil Saadatmandi reports financial support was provided by Ministero dell'Università e della Ricerca (Italy). The other authors declare that they have no known competing financial interests or personal relationships that could have appeared to influence the work reported in this paper.

Acknowledgment

The first author acknowledges the PhD grant received in application of the Italian Ministry Decree DM 1061/2021.

Appendix

Deduction of the loss sensitivity Eq. (6)

This section illustrates the details for the formulation of Eq. (6) with reference to a simple radial network example for a balanced case (Fig. A1). The branches are numbered as the ending nodes. The subscript t that represents the time step is dropped off for simplicity of notation. The relevant data are

the branch resistances R_1, R_2 and R_3. The shunt node currents are $\bar{I}_{S1}$, $\bar{I}_{S2}$, and $\bar{I}_{S3}$. The topology is represented by the matrix $\mathbf{\Gamma}$ (with nodes on the rows and branches on the columns).

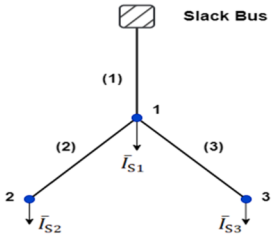

$$\mathbf{\Gamma} = |\mathbf{c}_1 \quad \mathbf{c}_2 \quad \mathbf{c}_3| = \begin{vmatrix} 1 & 0 & 0 \\ 1 & 1 & 0 \\ 1 & 0 & 1 \end{vmatrix}$$

$$\mathbb{B}_1 = \{1\}, \mathbb{B}_2 = \{1,2\}, \mathbb{B}_3 = \{1,3\}$$

Fig. A1. Radial network example with slack bus and three nodes

From the loss allocation Eq. (2), by collecting the terms with common entries, the total losses are expressed as:

$$\mathscr{L}_{\text{tot}} = \Re\text{e}\{R_1 I_{S1}^2 + R_1 I_{S2}^2 + R_1 I_{S3}^2 + R_2 I_{S2}^2 + R_3 I_{S3}^2 + R_1 I_{S1} I_{S2}\left(\text{e}^{\text{j}(\gamma_{S1}-\gamma_{S2})} + \text{e}^{\text{j}(\gamma_{S2}-\gamma_{S1})}\right) + R_1 I_{S1} I_{S3}\left(\text{e}^{\text{j}(\gamma_{S1}-\gamma_{S3})} + \text{e}^{\text{j}(\gamma_{S3}-\gamma_{S1})}\right) + R_1 I_{S2} I_{S3}\left(\text{e}^{\text{j}(\gamma_{S2}-\gamma_{S3})} + \text{e}^{\text{j}(\gamma_{S3}-\gamma_{S2})}\right)\} \quad \text{(A1)}$$

By taking the real part, considering the symmetry properties of the cosine function, the total losses become:

$$\mathscr{L}_{\text{tot}} = R_1\left(I_{S1}^2 + I_{S2}^2 + I_{S3}^2\right) + R_2 I_{S2}^2 + R_3 I_{S3}^2 + 2 \quad R_1 I_{S1} I_{S2} \cos(\gamma_{S1} - \gamma_{S2}) + 2 \quad R_1 I_{S1} I_{S3} \cos(\gamma_{S1} - \gamma_{S3}) + 2 \quad R_1 I_{S2} I_{S3} \cos(\gamma_{S2} - \gamma_{S3}) \quad \text{(A2)}$$

The loss sensitivities are calculated as the derivatives of the total losses with respect to the shunt node current amplitudes:

$$\frac{\partial \mathscr{L}_{\text{tot}}}{\partial I_{S1}} = 2 \quad R_1 I_{S1} + 2 \quad R_1 I_{S2} \cos(\gamma_{S2} - \gamma_{S1}) + 2 \quad R_1 I_{S3} \cos(\gamma_{S3} - \gamma_{S1})$$

$$\frac{\partial \mathscr{L}_{\text{tot}}}{\partial I_{S2}} = 2 \quad R_1 I_{S2} + 2 \quad R_2 I_{S2} + 2 \quad R_1 I_{S1} \cos(\gamma_{S1} - \gamma_{S2}) + 2 \quad R_1 I_{S3} \cos(\gamma_{S3} - \gamma_{S2})$$

$$\frac{\partial \mathscr{L}_{\text{tot}}}{\partial I_{S3}} = 2 \quad R_1 I_{S3} + 2 \quad R_3 I_{S3} + 2 \quad R_1 I_{S1} \cos(\gamma_{S1} - \gamma_{S3}) + 2 \quad R_1 I_{S2} \cos(\gamma_{S2} - \gamma_{S3}) \quad \text{(A3)}$$

The terms that contain the cosines are never multiplied by the current with respect to which the derivative is taken. As such, considering for example the derivative taken with respect to I_{Sk} and $i \neq k$, the term $I_{Si}\cos(\gamma_{Si} - \gamma_{Sk})$ is elaborated as $\Re\text{e}\{I_{Si}\text{e}^{\text{j}\gamma_{Si}}\,\text{e}^{-\text{j}\gamma_{Sk}}\} = \Re\text{e}\{\text{e}^{-\text{j}\gamma_{Sk}}\bar{I}_{Si}\}$.

By introducing the column vectors $\mathbf{c}_b$ and $\mathbf{i}_S$, the formulation of the loss sensitivity at node k for the balanced system is then:

$$\frac{\partial \mathscr{L}_{\text{tot}}}{\partial I_{Sk}} = \sum\nolimits_{b \in \mathbb{B}_k} 2R_b \mathbf{c}_b^{\text{T}}\, \Re\text{e}\{\text{e}^{-\text{j}\gamma_{Sk}}\mathbf{i}_S\} \quad \text{(A4)}$$

The formulation (A4) is written in the generalised form valid for any radial network and is used as Eq. (6) in this paper.

Loss sensitivity calculations for a two-node network example with voltage-dependent models

Let us consider a two-node system supplied at voltage $\bar{E}$ at the beginning of the line and with voltage $\bar{V}$ at the end of the line. The line parameters are the resistance R and the reactance X, from which the square of the impedance is $Z^2 = R^2 + X^2$. The system supplies a load that can be represented with the assigned current, assigned power, or assigned impedance model. Three cases of loss sensitivity calculations are shown, each one considering one of the models. In all the cases, the total line losses are expressed as $\mathscr{L}_{\text{tot}} = RI^2$. The expressions of I^2 are written in analytical form for the three models, then for each model the derivative of the total losses with respect to the relevant parameter is calculated.

Assigned power: the active power P and reactive power Q are assigned. The analytical formulation in terms of the current is given by the classical biquadratic equation

$$Z^2 I^4 - 2 \quad \left(\frac{E^2}{2} - (RP + XQ)\right) I^2 + P^2 + Q^2 = 0 \quad \text{(B1)}$$

from which, picking up the practically useful solution with the lower current (minus sign in front of the square root):

$$I^2 = \frac{1}{Z^2}\left(\frac{E^2}{2} - (RP + XQ) - \sqrt{\left(\frac{E^2}{2} - (RP + XQ)\right)^2 - Z^2\left(P^2 + Q^2\right)}\right) \quad \text{(B2)}$$

Replacing I^2 in the expression $\mathscr{L}_{\text{tot}} = RI^2$, the derivative of the total losses with respect to the active power is

$$\frac{d\mathscr{L}_{\text{tot}}}{dP} = -\frac{R^2}{Z^2} - \frac{R}{Z^2}\frac{\left(-2R\left(\frac{E^2}{2} - (RP + XQ)\right) - 2Z^2P\right)}{2\sqrt{\left(\frac{E^2}{2} - (RP + XQ)\right)^2 - Z^2\left(P^2 + Q^2\right)}} \quad \text{(B3)}$$

Assigned current: the relevant parameter for loss calculation is the current that corresponds to the active power P and reactive power Q, respectively, in the solution point with voltage amplitude V. The square of the current is needed to determine the losses:

$$I^2 = \frac{P^2 + Q^2}{V^2} \tag{B4}$$

From the expression $\mathscr{L}_{\text{tot}} = RI^2$, the derivative of the total losses with respect to the current amplitude is

$$\frac{d\mathscr{L}_{\text{tot}}}{dI} = 2 \quad R\,I \tag{B5}$$

Assigned impedance: the parameters are the resistance R_{d} and the reactance X_{d} that correspond to the active power P and reactive power Q, respectively, in the solution point with voltage amplitude V.

$$I^2 = \frac{E^2}{(R + R_{\text{d}})^2 + (X + X_{\text{d}})^2} \tag{B6}$$

From the expression $\mathscr{L}_{\text{tot}} = RI^2$, the derivative of the total losses with respect to the resistance R_{d} is

$$\frac{d\mathscr{L}_{\text{tot}}}{dR_{\text{d}}} = \frac{-2R(R + R_{\text{d}})E^2}{\left((R + R_{\text{d}})^2 + (X + X_{\text{d}})^2\right)^2} \tag{B7}$$

Data availability

Data will be made available on request.

References

[1] S. Bahramara, P. Sheikhahmadi, G. Chicco, Introduction to electrical system operation with distributed energy resources, grid services, and flexibility, in: Distribution System Modeling with Distributed Energy Resources, Chapter 1, Elsevier, 2025, pp. 1–14.

[2] L. Zhang, H. Ye, Y. Ge, Z. Li, Ramping-based variable-timescale Co-optimization for distribution planning and operation, IEEE Trans. Power Syst. 40 (3) (May 2025) 2519–2531.

[3] A. Demazy, T. Alpcan, I. Mareels, A probabilistic reverse power flows scenario analysis framework, IEEE Open Access J. Power Energy 7 (2020) 524–532.

[4] I.B. Majeed, N.I. Nwulu, Reverse power flow due to solar photovoltaic in the low voltage network, IEEE Access 11 (2023) 44741–44758.

[5] V. Umoh, J. Akpan, D. Donaldson, A.A. Adebiyi, Tools and test systems for hosting capacity assessment, in: H.H.H. Mousa, K. Mahmoud, M. Lehtonen (Eds.), Hosting Capacity Aspects in Distribution Networks Towards Sustainable Energy Systems, Chapter 7, Elsevier, 2025, pp. 151–171.

[6] L. Lukač, T. Antić, T. Capuder, Changing the paradigm of distribution networks planning and operation: a systematic review of the distributed energy resources impact, Sustain. Energy Grids Netw. 45 (2026) 102070.

[7] M.H.J. Bollen, F. Hassan, Power system performance, in: Integration of Distrib. Gener. in the Power Syst., 1st Ed., Chapter 3, Wiley & Sons, Hoboken, NJ, USA, 2011, pp. 84–101.

[8] Y. Cho, E. Lee, K. Baek, J. Kim, Stochastic optimization-based hosting capacity estimation with volatile net load deviation in distribution grids, Appl. Energy 341 (2023) 121075.

[9] P. Therapontos, S. Panagi, C.A. Charalambous, P. Aristidou, Coordinated curtailment of uncontrollable distributed energy resources in isolated power systems, Sustain. Energy Grids Netw. 45 (2026) 102124.

[10] Y. Su, F. Liu, Z. Wang, Y. Zhang, B. Li, Y. Chen, Multi-stage robust dispatch considering demand response under decision-dependent uncertainty, IEEE Trans. Smart Grid 14 (4) (Jul. 2023) 2786–2797.

[11] W. Kanchana, J.G. Singh, W. Ongsakul, Data-driven hidden solar PV and energy storage capacity estimation from the net-load of active distribution systems, Sustain. Energy Grids Netw. 44 (2025) 101940.

[12] M. Abujubbeh, B. Natarajan, Overview of loss sensitivity analysis in modern distribution systems, IEEE Access 10 (Feb. 2022) 16037–16051.

[13] O.I. Elgerd, The energy system in steady state – optimum operating strategies, in: Electric energy systems theory: an introduction, ch. 8, McGraw-Hill, New York, NY, USA, 1971, pp. 274–314.

[14] D.Q. Hun, N. Mithulananthan, Multiple distributed generator placement in primary distribution networks for loss reduction, IEEE Trans. Ind. Electron 60 (4) (Apr. 2013) 1700–1708.

[15] M. Abujubbeh, S. Munikoti, and B. Natarajan, Analytical power loss sensitivity analysis in distribution systems, in *Proc. IEEE Power & Energy Soc. General Meeting*, Washington, DC, USA, 2021.

[16] H.M. Ayres, D. Salles, W. Freitas, A practical second-order based method for power losses estimation in distribution systems with distributed generation, IEEE Trans. Power Syst. 29 (2) (Mar. 2014) 666–674.

[17] S. Wang, Q. Liu, X. Ji, A fast sensitivity method for determining line loss and node voltages in active distribution network, IEEE Trans. Power Syst. 33 (1) (Jan. 2018) 1148–1150.

[18] S.R. Vaishya, A.R. Abhyankar, P. Kumar, A novel loss sensitivity based linearized OPF and LMP calculations for active balanced distribution networks, IEEE Syst. J. 17 (1) (Mar. 2023) 1340–1351.

[19] J.R. Carson, Wave propagation in overhead wires with ground return, Bell Syst. Tech. J. N. Y. 5 (Oct. 1926) 539–554.

[20] M. Hong, An approximate method for loss sensitivity calculation in unbalanced distribution systems, IEEE Trans. Power Syst. 29 (3) (May 2014) 1435–1436.

[21] Y.J. Kim, Development and analysis of a sensitivity matrix of a three-phase voltage unbalance factor, IEEE Trans. Power Syst. 33 (3) (May 2018) 3192–3195.

[22] K. Ye, J. Zhao, C. Huang, N. Duan, Y. Zhang, T.E. Field, A data-driven global sensitivity analysis framework for three-phase distribution system with PVs, IEEE Trans. Power Syst. 36 (5) (Sep. 2021) 4809–4819.

[23] P. Chen, S. Liu, X. Wang, I. Kamwa, Physics-guided multi-agent deep reinforcement learning for robust active voltage control in electrical distribution systems, IEEE Trans. Circuits Syst. -I Regul. Pap. 71 (2) (Feb. 2024) 922–933.

[24] N. Shi, R. Cheng, L. Liu, Z. Wang, Q. Zhang, M.J. Reno, Data-driven affinely adjustable robust volt/var control, IEEE Trans. Smart Grid 15 (1) (Jan. 2024) 247–259.

[25] J. Wu, J. Yuan, Y. Weng, R. Ayyanar, Spatial-temporal deep learning for hosting capacity analysis in distribution grids, IEEE Trans. Smart Grid 14 (1) (Jan. 2023) 354–364.

[26] Y. Liang, J. Zhao, P. Siano, D. Srinivasan, Temporally-adaptive robust data-driven sparse voltage sensitivity estimation for large-scale realistic distribution systems with PVs, IEEE Trans. Power Syst. 38 (4) (Jul. 2023) 3977–3980.

[27] J. Chen, L.A. Roald, A data-driven linearization approach to analyze the three-phase unbalance in active distribution systems (art), Elect. Power Syst. Res. 211 (2022) 108573.

[28] M. Hong and K.A. Loparo, An Improved Electricity Market Model on Demand Response Considering Distribution Loss Sensitivities, in *Proc. IEEE Power & Energy Soc. General Meeting*, National Harbor, MD, USA, 2014.

[29] J.S. Savier, D. Das, Energy loss allocation in radial distribution systems: a comparison of practical algorithms, IEEE Trans. Power Del. 24 (1) (Jan. 2009) 260–267.

[30] K. Shaloudegi, N. Madinehi, S.H. Hosseinian, H.A. Abyaneh, A novel policy for locational marginal price calculation in distribution systems based on loss reduction allocation using game theory, IEEE Trans. Power Syst. 27 (2) (May 2012) 811–820.

[31] J. Mutale, G. Strbac, S. Curcic, N. Jenkins, Allocation of losses in distribution systems with embedded generation, IEE Proc. -Gener. Transm. Distrib. 147 (1) (Feb. 2000) 7–14.

[32] J.W. Bialek, Tracing the flow of electricity, IEE Proc. -Gener. Transm. Distrib. 143 (4) (Jul. 1996) 313–320.

[33] S. Tong, K.N. Miu, A network-based distributed slack bus model for DGs in unbalanced power flow studies, IEEE Trans. Power Syst. 20 (2) (May 2005) 835–842.

[34] A.J. Conejo, J.M. Arroyo, N. Alguacil, A.L. Guijarro, Transmission loss allocation: a comparison of different practical algorithms, IEEE Trans. Power Syst. 17 (3) (Aug. 2002) 571–576.

[35] E. Carpaneto, G. Chicco, J. Sumaili Akilimali, Characterization of the loss allocation techniques for radial systems with distributed generation, Elect. Power Syst. Res. 78 (8) (Aug. 2008) 1396–1406.

[36] A.J. Conejo, F.D. Galiana, I. Kockar, Z-bus loss allocation, IEEE Trans. Power Syst. 16 (1) (Feb. 2001) 105–109.

[37] J.S. Daniel, R.S. Salgado, M.R. Irving, Transmission loss allocation through a modified Ybus, IEE Proc. -Gener. Transm. Distrib. 152 (2) (Mar. 2005) 208–214.

[38] E. Carpaneto, G. Chicco, J. Sumaili Akilimali, Branch current decomposition method for loss allocation in radial distribution systems with distributed generation, IEEE Trans. Power Syst. 21 (3) (Aug. 2006) 1170–1179.

[39] P. Costa, M. Matos, Loss allocation in distribution networks with embedded generation, IEEE Trans. Power Syst. 19 (1) (Feb. 2004) 384–389.

[40] M. Atanasovski, R. Taleski, Energy summation method for loss allocation in radial distribution networks with DG, IEEE Trans. Power Syst. 27 (3) (Aug. 2012) 1433–1440.

[41] K.M. Jagtap, D.K. Khatod, Novel approach for loss allocation of distribution networks with DGs, Elect. Power Syst. Res. 143 (Feb. 2017) 303–311.
[42] S. Sharma, A.R. Abhyankar, Loss allocation for weakly meshed distribution system using analytical formulation of Shapley value, IEEE Trans. Power Syst. 32 (2) (Mar. 2017) 1369–1377.
[43] H. Kumar, D.K. Khatod, Loss allocation in three-phase distribution network using τ-value, IEEE Trans. Power Syst. 39 (3) (May 2024) 4924–4934.
[44] Z. Ghofrani-Jahromi, Z. Mahmoodzadeh, M. Ehsan, Distribution loss allocation for radial systems including DGs, IEEE Trans. Power Del. 29 (1) (Feb. 2014) 72–80.
[45] A.I. Nikolaidis, C.A. Charalambous, P. Mancarella, A graph-based loss allocation framework for transactive energy markets in unbalanced radial distribution networks, IEEE Trans. Power Syst. 34 (5) (Sep. 2019) 4109–4118.
[46] I. Bhand, S. Debbarma, Transaction-tracing based loss allocation in distribution networks under TE system, IEEE Syst. J. 15 (4) (Dec. 2021) 5664–5673.
[47] E. Carpaneto, G. Chicco, J. Sumaili Akilimali, Loss partitioning and loss allocation in three-phase radial distribution systems with distributed generation, IEEE Trans. Power Syst. 23 (3) (Aug. 2008) 1039–1049.
[48] M. Usman, M. Coppo, F. Bignucolo, R. Turri, A. Cerretti, Multi-phase losses allocation method for active distribution networks based on branch current decomposition, IEEE Trans. Power Syst. 34 (5) (Sep. 2019) 3605–3615.
[49] R. Verma, V. Sarkar, Active distribution network load flow analysis through non-repetitive FBS iterations with integrated DG and transformer modelling, IET Gener. Transm. Distrib. 13 (4) (Feb. 2019) 478–484.
[50] E. Bompard, E. Carpaneto, G. Chicco, R. Napoli, Convergence of the backward/forward sweep method for the load-flow analysis of radial distribution systems, Int. J. Elect. Power & Energy Syst. 22 (7) (Oct. 2000) 521–530.
[51] D. Shirmohammadi, H.W. Hong, A. Semlyen, G.X. Luo, A compensation-based power flow method for weakly meshed distribution and transmission networks, IEEE Trans. Power Syst. 3 (2) (May 1988) 753–762.
[52] W.H. Kersting, Series impedance of overhead and underground lines. Distribution system modeling and analysisch. 4, 4th ed., CRC Press, Boca Raton, FL, USA, 2018, pp. 77–119.
[53] F. Pilo, G. Pisano, S. Scalari, D. Dal Canto, A. Testa, R. Langella, R. Caldon, R. Turri, ATLANTIDE — digital archive of the Italian electric distribution reference networks, CIRED Workshop Integr. Renew. into Distrib. Grid (May 2012) 29–30.
[54] IEEE, The IEEE European Low Voltage test feeder. Accessed: 12 February 2025. [Online] Available: ⟨https://cmte.ieee.org/pes-testfeeders/resources/⟩.